MACROPHAGE SKEWING BY PHD2 HAPLODEFICIENCY PREVENTS ISCHEMIA BY INDUCING ARTERIOGENESIS

Yukiji Takeda[1,2,3,4], Sandra Costa[1,2,5#], Estelle Delamarre[1,2#], Carmen Roncal[1,2,3,4,6#], Rodrigo Leite De Oliveira[1,2,3,4], Mario Leonardo Squadrito[7], Veronica Finisguerra[1,2], Françoise Bruyère[3,4], Sofie Deschoemaeker[1,2], Mathias Wenes[1,2], Alexander Hamm[1,2], Jens Serneels[1,2], Julie Magat[8], Tapan Bhattacharrya[9], Andrey Anisimov[10], Benedicte F. Jordan[8], Kari Alitalo[10], Patrick Maxwell[9], Bernard Gallez[8], Zhenwu Zhuang[11], Yoshihiko Saito[12], Michael Simons[11], Michele De Palma[5] & Massimiliano Mazzone[1,2]

[1]Lab of Molecular Oncology and Angiogenesis, Vesalius Research Center, VIB, Leuven, Belgium; [2]Lab of Molecular Oncology and Angiogenesis, Vesalius Research Center, K.U.Leuven, Leuven, Belgium; [3]Lab of Angiogenesis and Neurovascular link, Vesalius Research Center, VIB, Leuven, Belgium; [4]Lab of Angiogenesis and Neurovascular link, Vesalius Research Center, K.U.Leuven, Belgium; [5]Life and Health Sciences Research Institute, Minho University, Braga, Portugal; [6]Atherosclerosis Research Laboratory, CIMA-University of Navarra, Pamplona, Spain; [7]Angiogenesis and Tumor Targeting Unit, HSR-TIGET and Vita-Salute University, San Raffaele Institute, Milan, Italy; [8]Biomedical Magnetic Resonance Unit, Medicinal Chemistry and Radiopharmacy U.C.Louvain, Brussels, Belgium; [9]Rayne Institute, University College London, London, UK; [10]Molecular/Cancer Biology Laboratory, Research Programs Unit, Institute for Molecular Medicine, Helsinki, Finland; [11]Cardiovascular Medicine, Yale University, New Haven, CT, USA; [12]The First Department of Internal Medicine, Nara Medical University, Nara, Japan; [#]These authors contributed equally to this work.

Editorial correspondence: Massimiliano Mazzone, Ph.D.
Vesalius Research Center, VIB, KULeuven,
Campus Gasthuisberg, Herestraat 49,
B-3000, Leuven, Belgium;
Tel: +32-16-34.61.76; fax: +32-16-34.59.90
e-mail: massimiliano.mazzone@vib-kuleuven.be

SUMMARY

PHD2 serves as oxygen sensor that rescues blood supply by regulating vessel formation and shape in case of oxygen shortage. However, it is unknown whether PHD2 can influence arteriogenesis. By using hindlimb ischemia as a model, we studied the role of PHD2 in collateral artery growth, a process that compensates the lack of blood flow in case of major arterial occlusion. Here, we show that $PHD2^{+/-}$ mice displayed preformed collateral arteries that ameliorated limb perfusion and prevented ischemic necrosis. The improved arteriogenesis in $PHD2^{+/-}$ mice was due to the expansion of circulating and tissue-resident Tie2-expressing monocytes/macrophages (TEMs) and their enhanced release of PDGFB and SDF1, resulting in increased smooth muscle cell recruitment and growth. This program relied on activation of the canonical NF-κB pathway in $PHD2^{+/-}$ mononuclear phagocytes. These results show how PHD2 controls blood flow and thus tissue oxygenation by skewing the macrophage towards an arteriogenic phenotype in ischemia.

INTRODUCTION

Vascular stenosis reduces blood supply resulting in ischemia, which causes tissue dysfunction and demise. This condition is however associated with the formation of new blood vessels (angiogenesis) and remodeling of preexisting collateral arterioles (arteriogenesis) that reestablish blood flow to the downstream tissue[1-3]. Spontaneous angiogenesis and arteriogenesis thus attenuate local tissue ischemia and improve the clinical outcome of the disease[2,4,5]. Upon occlusion of an artery, the blood flow is redirected into preexisting arteriolar anastomoses, causing enhanced shear stress on the endothelium of the collateral circulation[6-8]. As a consequence, endothelial cells (ECs) secrete VEGF, which induces the production of monocyte chemotactic protein-1 (CCL2/MCP1) from the endothelium itself and from adjacent smooth muscle cells (SMCs), leading to monocyte recruitment[2,7,9,10]. Once in the periarteriolar region, monocyte-derived macrophages produce growth factors that enhance the motility and proliferation of SMCs, as well as proteases that digest the extracellular matrix to provide space for new SMCs[2,8]. Recent studies have analyzed the functional plasticity of mononuclear phagocytes in response to different environmental cues. For instance, in cancer and atherosclerosis, macrophages generally display an "*alternatively activated*" (M2) phenotype[11,12], which enhances debris scavenging, angiogenesis, tissue remodeling, wound healing, and the promotion of type II immunity. On the other hand, in inflamed tissues, macrophages display a "*classically activated*" (M1) phenotype, which facilitates eradication of invading microorganisms and the promotion of type I immune responses[11,12]. However, macrophage heterogeneity during ischemia-induced arteriogenesis has not been elucidated yet. Although initiation of arteriogenesis by macrophages takes place in a non-hypoxic environment distant from the ischemic area[13,14], some of the cytokines that stimulate arteriogenesis are under the control of the prolyl hydroxylase domain protein PHD2[15,16]. PHD2 belongs to a larger family of proteins that utilize oxygen to hydroxylate the hypoxia-inducible transcription factors (HIF)-1α and HIF-2α and, thereby, target the latter for proteasomal degradation and hence inactivation[17]. In hypoxic conditions, PHDs are inactive, which allows HIFs to become stabilized and mount an adaptive response to hypoxia. Besides negatively regulating HIF accumulation, PHDs display a repressive role

in controlling the activity of NF-κB, a key signaling molecule for inflammation[18]. The control of NF-κB by PHDs can be both dependent and independent of the hydroxylase activity and therefore from the presence of oxygen used as a substrate[15,19-21].

Pharmacological inhibition, silencing, or genetic inactivation of PHD2 after birth stimulates angiogenesis and therapeutic revascularization through upregulation of angiogenic factors from the parenchymal tissue[16,22-24]. Recently, we have shown that heterozygous deficiency of PHD2 in ECs does not affect vessel density or lumen size, but normalizes their endothelial lining, barrier, and stability, thus resulting in increased blood vessel perfusion in tumors[25]. However, whether and how PHD2 plays a role in the regulation of the arteriogenic process remains enigmatic. By using hindlimb ischemia as a model of arteriogenesis, we found that reduced PHD2 levels in macrophages increases the production of arteriogenic cytokines, including SDF1 and PDGFB, in an NF-κB dependent manner. An increase of Tie2-expressing monocytes/macrophages (TEMs) in the blood and tissues accounts for the superior arteriogenesis in PHD2 haplodeficient mice. As a consequence of TEMs' production of SDF1 and PDGFB, the remodeling of collateral anastomoses is enhanced, thus conferring protection against ischemic damage. Altogether, these data indicate that a reduction of PHD2 levels in monocytes/macrophages unleashes NF-κB signals that skew their polarization towards an arteriogenic phenotype.

RESULTS

PHD2 HAPLODEFICIENCY PRESERVES TISSUE PERFUSION AND VIABILITY IN ISCHEMIA

We recently showed that stromal haplodeficiency of PHD2 increases tumor perfusion[25]. Prompted by these results, we examined whether partial loss of PHD2 also enhances perfusion of ischemic tissues. We therefore subjected mice to femoral artery ligation, an established procedure that reduces perfusion of the lower limb and causes ischemia in the calf (i.e. crural muscle). Laser-doppler measurements revealed that perfusion of the lower hindlimb was higher in $PHD2^{+/-}$ than wild-type (WT) mice 12, 24 and 48 hours after femoral artery ligation, during the critical period when myofibers die if they do not receive sufficient oxygen (Figure 1A). The increased perfusion in $PHD2^{+/-}$ mice translated into enhanced physical endurance in ischemic conditions (12 hours post-ligation), whereas both genotypes exhibited similar running capacity at baseline (Figure 1B). Quantification of oxygen levels in the calf by MRI-based oxymetry 12 hours after ligation revealed that femoral occlusion induced a drop of oxygen tension by 66% in WT and 46% in $PHD2^{+/-}$ mice (Figure 1C-E). Such differences in oxygen tension have been shown to influence the outcome of the ischemic disease[26]. Staining for the hypoxia-marker pimonidazole showed that the hypoxic area in the crural muscle of ligated limbs was 37.1 ± 3.0% in WT mice but only 16.0 ± 7.0% in $PHD2^{+/-}$ mice (Figure 1H-J). Pimonidazole staining of baseline WT and $PHD2^{+/-}$ crural muscles was negative (Figure 1F,G). In accordance with findings that oxygen consumption in conditions of low oxygen availability is associated with formation of reactive oxygen species (ROS), WT but not $PHD2^{+/-}$ crural muscles at 12 hours post-ligation stained strongly for 8-hydroxy-2-deoxyguanosine (8-OHdG), a marker of deoxyguanosine oxidation (Supplementary Figure 1C-E). At baseline, oxidative stress in the crural muscle was comparable in both genotypes (Supplementary Figure 1A,B,E). We next determined whether the decreased drop in perfusion and thus oxygen tension in $PHD2^{+/-}$ ligated limbs prevented ischemic necrosis. Histological analysis of the crural muscle (i.e. soleus) showed extensive ischemic damage in WT mice 72 hours after ischemia (Figure 1K). In $PHD2^{+/-}$ mice, ischemic necrosis of the soleus was reduced by more than 50% (Figure 1K-M). In accordance, crural muscle viability after ischemia was almost double in $PHD2^{+/-}$ than in WT mice (Figure 1N-P). Compared to WT mice, muscle

fibers in PHD2$^{+/-}$ mice also showed fewer signs of regeneration as assessed by BrdU staining, confirming that they were less damaged (Supplementary Figure 1F-H).

Upon femoral artery ligation, growth factors released by the ischemic crural muscle promote angiogenesis[1,27]. Indeed, in WT mice, 14 days after femoral artery occlusion, vessel density and total vessel area in near-completely regenerated regions of the soleus (an oxidative unit of the crural muscle) were increased respectively by 33% and 70% (Supplementary Figure 1I,J). In contrast, in PHD2$^{+/-}$ mice, these parameters remained unchanged compared to the baseline, likely because these muscles never experienced sufficient ischemia to stimulate angiogenesis (Supplementary Figure 1I,J).

We also wanted to assess whether PHD2$^{+/-}$ mice were protected against myocardial ischemia and therefore performed ligation of the left anterior descending coronary artery of WT and PHD2$^{+/-}$ hearts. The infarcted area was measured in desmin stained cross-sections 24 hours after coronary ligation. Desmin-negative area (a readout of cardiomyocyte death) was about 60% of the left ventricle in WT hearts and only 40% in PHD2$^{+/-}$ hearts (Figure 1Q-S). Compared to WT, PHD2$^{+/-}$ hearts displayed higher perfusion in both the infarcted and remote myocardium (Figure 1T-W).

Thus, PHD2 haplodeficiency greatly preserves perfusion and reduces tissue damage in ischemia.

PHD2 HAPLODEFICIENCY ELICITS "COLLATERAL VESSEL PRECONDITIONING"

Since PHD2$^{+/-}$ muscles were protected against ischemic damage already 12 hours after femoral artery ligation, we hypothesized that PHD2 haplodeficient mice were preadapted to and therefore capable of better tolerating the ischemic insult. The number and caliber of preexisting collaterals (primary, secondary, and tertiary branches) are major determinants of the severity of tissue injury in occlusive diseases since these conduits allow blood flow to bypass the obstruction[2,4,5]. We therefore investigated whether PHD2$^{+/-}$ mice showed increased collaterals at baseline, independently of ischemia. Macroscopic counting of collateral arteries on gelatin-bismuth angiographies in the thigh of non-occluded limbs revealed a similar number of primary branches in both genotypes (Figure 2A,B). PHD2$^{+/-}$ mice however, had 1.7 and 2 fold more secondary and tertiary collateral arteries, respectively (Figure 2A-D). Histological analysis of the adductor muscles (located

in the inner thigh, where collaterals form) showed that the total area and density of bismuth-positive collaterals at baseline were respectively 2.0 and 2.3 fold higher in $PHD2^{+/-}$ than WT mice (Figure 2E-H). In contrast, capillary density and area in the adductor were comparable in both genotypes (Supplementary Figure 2A,B). Consistent with these results, X-ray radiography (Figure 2I,J) and micro-CT scans showed a higher number of large vessels (>200 μm in diameter) in $PHD2^{+/-}$ than WT thighs at baseline (Figure 2K-M), whereas smaller vessels (<200 μm in diameter) were not changed (Supplementary Figure 2C). Similar results were obtained in $PHD2^{+/-}$ hearts at baseline, displaying a higher density of large vessels (Figure 2N-P), and a similar number of small vessels and capillaries, compared to WT (Supplementary Figure 2D,E).

After femoral artery ligation, evaluation of gelatin-bismuth angiographies in WT limbs showed a 30% induction of the collateral vascularization 12 and 72 hours post-ischemia (Figure 2C,D). Conversely, in $PHD2^{+/-}$ mice the number of collaterals in the adductor did not significantly change after occlusion, likely because they were already expanded at baseline (Figure 2C,D). Nevertheless, there were still more secondary and tertiary collateral branch arteries after ischemia in $PHD2^{+/-}$ than WT mice (Figure 2C,D). Histological analysis confirmed that 12 and 72 hours post-ligation, the bismuth-positive collateral area and density in adductor muscles were still higher in $PHD2^{+/-}$ than in WT controls (Figure 2G,H).

To increase blood flow, collateral vessels undergo extensive remodeling (arteriogenesis) and thus the tunica media, consisting of α-smooth muscle actin (αSMA)-positive contractile SMCs, becomes thicker and the diameter of the conduit enlarges. Staining of adductor tissue sections for αSMA revealed that number and total area of αSMA^{+} collateral vessels were respectively 1.5 and 2 times increased in $PHD2^{+/-}$ muscles at both baseline and after ischemia (Figure 2Q,R). However, the mean area of αSMA^{+} collaterals was higher in $PHD2^{+/-}$ than WT mice only at baseline, since, 72 hours post-ligation, WT collaterals enlarged to the same size as $PHD2^{+/-}$ collaterals (Figure 2S,U-Y). A similar trend was observed by measuring the thickness of the tunica media (Figure 2T). These data show that, at baseline, the collateral vessels of $PHD2^{+/-}$ mice were similar to those of WT mice after femoral artery ligation. This “collateral vessel preconditioning” offered $PHD2^{+/-}$ mice a remarkable protection against lethal muscle ischemia.

PHD2$^{+/-}$ MACROPHAGES DISPLAY A SPECIFIC PHENOTYPE

Since inflammatory cells and in particular macrophages are known to produce SMC/EC-mitogens, cytokines and proteases during collateral growth, we expected that the increased collateralization in PHD2$^{+/-}$ muscles was due to enhanced infiltration of leukocytes in response to HIF-mediated release of chemoattractant proteins[28]. Surprisingly, when we measured the density of leukocytes and macrophages by staining adductor tissue sections for CD45 and F4/80, respectively, there was no difference between both genotypes at baseline (Figure 3A,B). Ligation of the femoral artery induced a significant, but comparable increase in inflammatory cell accumulation in WT and PHD2$^{+/-}$ adductors. Consistently, RNA levels of MCP1, one of the most important proinflammatory cytokines in limb ischemia[2,7,9,10], did not differ in the two genotypes either at baseline or after femoral artery occlusion (Supplementary Figure 3A).

We therefore explored whether the phenotype, not the quantity, of the infiltrating macrophages was different in PHD2$^{+/-}$ and WT mice. We measured the density of wound-healing/proangiogenic macrophages, which can be identified by their enhanced expression of the mannose receptor, MRC1/CD206[29-31], and correspond to M2-polarized macrophages[11,12]. Notably, costaining adductor sections for MRC1 and the macrophage specific marker F4/80 revealed that the number of F4/80^{+}MRC1^{+} cells was augmented by 75% at baseline conditions in PHD2$^{+/-}$ as compared to WT mice (Figure 3C-E). Seventy-two hours after ligation, their numbers were increased by 95% in WT mice and by 54% in PHD2$^{+/-}$ mice, but remained higher by 35% in ischemic PHD2$^{+/-}$ than WT mice (Figure 3C,F,G).

Prompted by these results, we gene-profiled WT and PHD2$^{+/-}$ macrophages collected by peritoneal lavage (peritoneal macrophages, pMØ) and analyzed the expression level of proangiogenic/proarteriogenic, proinflammatory, and antiangiogenic genes. Remarkably, the genes that were upregulated in PHD2$^{+/-}$ macrophages were markers of wound-healing/proangiogenic (i.e. M2-like) macrophages[11,29] and comprised Tie2, Arg1, CXCR4, CCR2, Nrp1, HGF, MMP2, FIZZ, CXCL12/SDF1, PDGFB, and TGFβ (Figure 3H). Of note, most of these molecules have been reported to play an important role during the arteriogenic process[6,32-36]. Conversely, several proinflammatory or antiangiogenic (i.e. M1-type) molecules were downregulated in PHD2$^{+/-}$ macrophages;

these included IL1ß, IL6, NOS2, and IL12 (Figure 3H). The changes in the molecular signature of macrophages were already detectable at baseline conditions, since F4/80^{+} cells freshly sorted from adductor muscles of PHD2$^{+/-}$ mice expressed higher levels of PDGFB, SDF1, Tie2, MMP2, Nrp1 (Figure 3I). After 72 hours of ischemia, the expression levels of these markers caught up in WT tissue macrophages (Figure 3I). Interestingly, in ischemia, PHD2 levels were reduced by almost 50% in WT macrophages while they were half in PHD2$^{+/-}$ macrophages both at baseline and after ischemia (versus WT macrophages at baseline; Figure 3I). No differences were detected in WT and PHD2$^{+/-}$ ECs, freshly isolated from adductor muscles at baseline and in ischemia (Supplementary Table 1). Thus, PHD2$^{+/-}$ macrophages display a unique and cell specific gene signature, which is reminiscent, at least in part, of M2-polarized macrophages[11,29,30,37].

HETEROZYGOUS DEFICIENCY OF PHD2 IN MYELOID CELLS PREVENTS ISCHEMIC DAMAGE

To investigate whether reduced levels of macrophage-derived PHD2 displays collateral vessel preconditioning and thus protection against ischemia, we generated conditional PHD2 deficient mice lacking one or two PHD2 alleles specifically in myeloid cells (PHD2$^{LysCre;lox/wt}$ and PHD2$^{LysCre;lox/lox}$ respectively) by intercrossing PHD2$^{lox/wt}$ and PHD2$^{lox/lox}$ mice with LysM:Cre mice expressing the Cre-recombinase under the control of the myeloid-specific lysozyme M promoter[38]. In contrast to PHD2 knockout mice, which die between E12.5 and E14.5 due to placental defects[25,39], mice with homozygous deficiency of PHD2 in myeloid cells (PHD2$^{LysCre;lox/lox}$) are viable and fertile. Gelatin-bismuth angiographies revealed a higher number of secondary and tertiary collateral branch arteries in heterozygous PHD2$^{LysCre;lox/wt}$ mice while arterialization was unchanged in PHD2$^{LysCre;lox/lox}$ mice (Figure 4A,B). This was likely due to compensatory activity of PHD3 in PHD2$^{LysCre;lox/lox}$ macrophages (see below). Histological analysis of the same adductor samples showed that the total area and density of bismuth positive collaterals were higher in PHD2$^{LysCre;lox/wt}$, but not in PHD2$^{LysCre;lox/lox}$ mice compared to control mice (Figure 4C,D). Collateral vessel preconditioning conferred protection against ischemia since, 72 hours after femoral artery occlusion, muscle necrosis was reduced by 67% in PHD2$^{LysCre;lox/wt}$, but not in PHD2$^{LysCre;lox/lox}$ mice (Figure 4E-H). Similarly, in ischemia, the running capacity of PHD2$^{LysCre;lox/wt}$, but not of PHD2$^{LysCre;lox/lox}$ mice was 1.6-fold higher compared to PHD2$^{LysCre;wt/wt}$ mice while comparable at baseline (Figure 4I).

To further explore whether the increased arteriogenesis in PHD2 haplodeficient mice could be attributed to the lack of one PHD2 allele in macrophages, we transplanted WT or $PHD2^{+/-}$ (hereafter HE for "heterozygous") bone marrow of syngenic mice, ubiquitously expressing GFP, into lethally irradiated WT recipients (referred to as WT→WT and HE→WT mice, respectively) or into lethally irradiated $PHD2^{+/-}$ recipients (referred to as WT→HE and HE→HE mice, respectively). Collateral arteries were quantified 5 weeks after bone marrow transplantation, when hematopoietic reconstitution by GFP^+ blood cells was, on average, 82 ± 8% and differential white blood counts were comparable in all the groups (not shown). Histological analysis of gelatin-bismuth-based angiographies revealed greater numbers and area of collateral vessels in HE→WT than WT→WT mice, while not differing from HE→HE mice, supporting the key role of bone marrow derived cells in enhancing collateralization (Figure 4J,K). Interestingly, collateral vessel parameters in WT→WT and WT→HE mice were comparable (Figure 4J,K), indicating that bone marrow derived cells are also important to sustain preexisting arteries in PHD2 heterozygous mice. In accordance, ischemic necrosis at 72 hours post-ligation was prevented in HE→HE and HE→WT mice, while it did not reach statistical significance in WT→HE mice (Figure 4L). We also assessed whether transplantation of HE bone marrow into lethally irradiated WT recipients would suffice to improve the physical endurance in ischemia. In a treadmill test, the running capacity of HE→WT mice was twice as good as in WT→WT mice 12 hours after femoral artery ligation while no differences were detected at baseline (Figure 4M).

Finally, we generated another strain lacking one PHD2 allele in both the hematopoietic and endothelial lineage ($PHD2^{Tie2Cre;lox/wt}$) by using the Tie2:Cre deleter mouse line[25,40]. Reciprocal bone marrow transplantation of $PHD2^{Tie2Cre;lox/wt}$ and $PHD2^{Tie2Cre;wt/wt}$ mice revealed that increased arteriogenesis of PHD2 heterozygous mice was specifically caused by loss of one PHD2 allele in bone marrow derived hematopoietic cells, but not in endothelial cells (Supplementary Table 2). Reduction of collateral branches in $PHD2^{Tie2Cre;lox/wt}$ recipient mice transplanted with a WT bone marrow ($PHD2^{Tie2Cre;wt/wt}$) further supported the concept that PHD2 heterozygous macrophages are required not only to trigger arteriogenesis but also to preserve existing arteries (Supplementary Table 2). Deletion of one PHD2 allele selectively in ECs or SMCs did not affect arteriogenesis (Supplementary Table 3). Thus, lower levels of PHD2 in bone marrow derived myeloid cells, but not in ECs and/or SMCs, increase collateral vessel formation

and prevent ischemic damage.

MACROPHAGE-DERIVED SDF1 AND PDGFB PROMOTE ARTERIOGENESIS

In order to unravel the biological mechanism underlying the arteriogenic phenotype, we assessed how WT and PHD2$^{+/-}$ macrophages affect the behavior of ECs and SMCs, the two main cellular components of arteries. First, we evaluated the chemotactic potential of primary ECs and SMCs towards WT and PHD2$^{+/-}$ macrophages. EC migration towards WT or PHD2$^{+/-}$ macrophages was comparable and 50-times higher than towards culture medium alone (Figure 5A-D). SMCs migrated only 6.5-times more efficiently when WT macrophages were seeded in the lower chamber of the transwell (compared to control medium), whereas migration towards PHD2$^{+/-}$ macrophages was 44-times higher (Figure 5E-H). Given the established role of SDF1 and PDGFB in the recruitment of SMCs and/or SMC progenitors[41-43] and the aforementioned finding that these two cytokines were upregulated the highest in PHD2$^{+/-}$ macrophages (see Figure 3H), we tested whether inhibiting these pathways, alone or in combination, would abrogate chemoattraction of SMCs towards PHD2$^{+/-}$ macrophages. Combined inhibition of SDF1 and PDGFB signaling by AMD3100 and imatinib, respectively, abrogated the increased migration of SMCs towards PHD2$^{+/-}$ macrophages, while either treatment alone was not effective (Figure 5I). Similarly, when silencing both SDF1 and PDGFB in PHD2$^{+/-}$ macrophages, SMC migration was almost completely prevented, though each shRNA alone was already partly effective (Supplementary Figure 4A and Supplementary Note 1).

To assess the influence of soluble factors released by WT and PHD2$^{+/-}$ macrophages on EC and SMC growth, we performed a cell viability assay. We seeded ECs or SMCs on the upper side of a 0.4 µm-pore filter (that does not allow cell migration but only protein diffusion), and WT or PHD2$^{+/-}$ macrophages in the lower chamber. Notably, growth of SMCs was enhanced by soluble factors released from PHD2$^{+/-}$ (versus WT) macrophages (Figure 5J). EC growth was not differently affected by WT and PHD2$^{+/-}$ macrophages (Figure 5K). SMCs display a proliferative (or synthetic) phenotype during the phase of active growth in contrast to the contractile phenotype in mature vessels[44]. The proliferative or synthetic phenotype is characterized by the reduction of contractile proteins including smoothelin, NmMHC, αSMA, and of calponin family proteins, i.e. calponin-1 and

Sm22α[44, 45]. The down-modulation of these genes in SMCs indicates that these cells are under the influence of growth factors and are able to migrate and to proliferate. Consistent with the enhanced growth of SMCs seeded in the presence of PHD2$^{+/-}$ macrophages, conditioned medium from PHD2$^{+/-}$ macrophages reduced the expression level of calponin-1, SM22α, smoothelin, NmMHC and αSMA, therefore supporting a proliferative phenotype (Figure 5L-P). Unlike what we observed in the migration assays, AMD3100 or imatinib alone abrogated the increased SMC growth by PHD2$^{+/-}$ macrophages. The combination of both AMD3100 and imatinib did not elicit an additive effect (Figure 5Q). Similarly, both single and combined knockdown of SDF1 and PDGFB in PHD2$^{+/-}$ macrophages hindered SMC growth (Supplementary Figure 4B).

Prompted by the in vitro results, we treated WT→WT and HE→WT mice with daily administration of AMD3100 (5 mg/kg) or imatinib (50 mg/kg), alone or in combination. In vivo, each drug alone only partially prevented the increased formation of second generation collateral branches in HE→WT mice (Figure 5R), while third generation collaterals were affected by either treatment alone (Figure 5S). However, the combination of AMD3100 and imatinib more potently prevented collateralization in the adductor of these mice. In WT→WT mice, the number of collateral branch arteries was not affected in all conditions tested (Figure 5R,S). Thus, in mice with reduced level of myeloid PHD2, combined PDGFB and SDF1 pathway activation is necessary to complete the arteriogenic process.

MACROPHAGES PROMOTING ARTERIOGENESIS IN PHD2$^{+/-}$ MICE ARE TEMS

Tie2 is a gene recently found to be significantly upregulated in a subpopulation of macrophages, known as TEMs, which express an M2-like, wound healing / proangiogenic phenotype[29-31,46]. Although TEMs express genes that are commonly expressed by other macrophage subsets (including PDGFB), they display greatly enhanced expression of SDF1[29]. Since Tie2 was strongly induced in PHD2$^{+/-}$ macrophages, we explored if this increase was due to an enhanced fraction of TEMs in the total macrophage population. As tumor TEMs express MRC1 to higher levels than classically activated macrophages / inflammatory macrophages[29,31] and because we found that PHD2$^{+/-}$ adductors display enhanced infiltration of F4/80^{+}MRC1^{+} macrophages (Figure 3C), we stained adductor

sections from WT and PHD2$^{+/-}$ mice for F4/80, MRC1 and Tie2 in order to rigorously identify TEMs. At baseline, F4/80^{+}MRC1^{+}Tie2^{+} TEMs were scarce in WT mice but were 4-times more abundant in PHD2$^{+/-}$ mice (Figure 6A). Seventy-two hours after femoral artery occlusion, the density of TEMs was 3.2-times higher in WT but 1.3-fold increased in PHD2$^{+/-}$ mice towards the baseline (Figure 6A). Thus, TEM density was still 1.6-fold higher in ischemic PHD2$^{+/-}$ than WT mice (Figure 6A). The increased presence of tissue-resident TEMs in PHD2$^{+/-}$ than WT mice was not due to a differential expression of the Tie2 ligands, angiopoietin-1 and angiopoietin-2, since transcript levels of these two cytokines were similar in WT and PHD2$^{+/-}$ adductors at baseline and ischemic conditions (Supplementary Figure 3B,C). When we measured Tie2-expressing monocytes (gated as CD115^{+}Tie2^{+} leukocytes) in the blood, we found a 3.4-fold higher TEM frequency in PHD2$^{+/-}$ than WT mice at baseline (Figure 6B). Interestingly, 72 hours after femoral artery ligation, the frequency of circulating TEMs was reduced by 3.4-fold in WT and 2.2-fold in PHD2$^{+/-}$ mice, although this decrease reached statistical significance in WT mice only (Figure 6B). Similar results were observed when quantifying the transcript levels of Tie2 in WT and PHD2$^{+/-}$ CD115^{+} circulating monocytes, though the overall expression of Tie2 was low (Figure 6C). In F4/80^{+} tissue macrophages, Tie2 transcripts were almost 100-times higher than in monocytes. After ligation, Tie2 transcript levels were further augmented, but only in WT macrophages, likely because PHD2$^{+/-}$ macrophages presented increased Tie2 expression already at baseline (Figure 6C). In mice, expression of Gr1 distinguishes “inflammatory” monocytes (CD115^{+}Gr1^{high}) from “resident” monocytes (CD115^{+}Gr1$^{low/neg}$)[47,48]. As previously reported[29], circulating TEMs in PHD2$^{+/-}$ mice are mostly CD115^{+}Gr1$^{low/neg}$ (Supplementary Figure 5). Altogether, these data suggest that, in ischemia, TEMs are recruited from the blood to the adductor where they trigger arteriogenesis.

To address if TEMs are functionally involved in the maturation of collateral arteries and thus preadaptation to ischemia in PHD2$^{+/-}$ mice, we used a 'suicide' gene strategy based on the *Herpes simplex* virus (HSV) thymidine kinase (tk)-ganciclovir (GCV) system[49]. We transplanted mice with WT or PHD2$^{+/-}$ bone marrow-derived lineage-negative cells transduced with a lentiviral vector (LV) expressing the HSV-tk cDNA under the control of the Tie2 promoter/enhancer (Tie2:tk-BMT mice; Supplementary Note 2). By this approach, bone marrow-derived TEMs can be specifically eliminated upon GCV

administration in the transplanted mice (Supplementary Note 3). GCV-treated and untreated mice were monitored for arterial growth at baseline as well as 3 and 7 days after ligation by staining adductor sections for αSMA. GCV-untreated $PHD2^{+/-}$ Tie2:tk-BMT mice displayed increased number of αSMA^{+} arteries and this density only slightly augmented at 3 and 7 days after ischemia. Remarkably, the arterial vessel preconditioning was completely abolished in GCV-treated $PHD2^{+/-}$ Tie2:tk-BMT mice and thus protection against ischemia was lost at both 3 and 7 days post-ligation (Figure 6D,E). In WT mice, TEM depletion by GCV administration prevented ischemia-induced arteriogenesis and consequent tissue healing 7 days post-ligation (Figure 6D,E). Thus, TEMs fuel arteriogenesis in $PHD2^{+/-}$ mice at baseline and in WT mice during ischemia.

ACUTE DELETION OF PHD2 FAVORS TEMS, ARTERIOGENESIS AND ISCHEMIA PROTECTION

In order to strengthen the possible therapeutic value of our findings, we assessed whether acute deletion of PHD2 in macrophages induced arteriogenesis and protection against ischemia as observed in $PHD2^{+/-}$ mice. To this end, we generated tamoxifen-inducible PHD2 haplodeficient mice ($PHD2^{Rosa26CreERT;lox/wt}$) where the Rosa26 promoter directs the ubiquitous expression of the fusion protein Cre-ERT2. Administration of 4-hydroxytamoxifen to $PHD2^{Rosa26CreERT;lox/wt}$ peritoneal macrophages induced a 50% reduction of PHD2 levels and increased the expression of PDGFB, SDF1, and Tie2, therefore resembling the phenotype of $PHD2^{+/-}$ macrophages (Supplementary Figure 6A). To address whether acute deletion of PHD2 in macrophage fuels arteriogenesis, bone marrows from $PHD2^{Rosa26CreERT;lox/wt}$ mice were transplanted into lethally irradiated WT recipient mice ($HE^{Rosa26CreERT}$→WT). After five weeks, transplanted mice were treated with vehicle or tamoxifen (1 mg/mouse for 5 days). Fourteen days after tamoxifen treatment, circulating TEMs were almost 3-fold higher (Supplementary Figure 6B) and both secondary and tertiary collateral branches were respectively 1.6 and 2.3 times more abundant than in vehicle-treated mice (Supplementary Figure 6C). Consistent with an increased arteriogenesis, ischemic damage in tamoxifen-treated $HE^{Rosa26CreERT}$→WT mice was greatly reduced (Supplementary Figure 6D). These data suggest that acute inactivation of PHD2 might represent a preventive medicine for ischemic diseases.

HETEROZYGOUS DEFICIENCY OF PHD2 IN MACROPHAGES ENHANCES NF-κB ACTIVITY

PHD2 oxygen sensor negatively regulates HIF accumulation and NF-κB activity[15,25]. When analyzing the accumulation of HIF-1α and HIF-2α by Western blot analysis, we observed that the levels of HIF-1α and HIF-2α in PHD2 haplodeficient macrophages ($PHD2^{LysCre;lox/wt}$) were comparable to the control ($PHD2^{LysCre;wt/wt}$). In contrast, HIF-1α and HIF-2α levels in PHD2 null macrophages ($PHD2^{LysCre;lox/lox}$) were respectively 4 and 2 times higher than in control macrophages ($PHD2^{LysCre;wt/wt}$; Figure 6F). We therefore quantified NF-κB activity by transducing $PHD2^{LysCre;lox/wt}$, $PHD2^{LysCre;lox/lox}$, $PHD2^{LysCre;wt/wt}$ macrophages with a lentiviral vector carrying an NF-κB-responsive firefly luciferase reporter (Figure 6G). Interestingly, NF-κB activity was increased by 65% in PHD2 haplodeficient macrophages but unaffected in PHD2 null macrophages.

We hypothesized that other PHD oxygen sensors might compensate for the complete loss of PHD2. We therefore measured RNA levels of PHD1, PHD2, and PHD3 in $PHD2^{LysCre;wt/wt}$, $PHD2^{LysCre;lox/wt}$ and $PHD2^{LysCre;lox/lox}$ macrophages. While PHD2 levels were decreased by 40% and 93% in $PHD2^{LysCre;lox/wt}$ and $PHD2^{LysCre;lox/lox}$ macrophages, respectively, PHD1 and PHD3 transcript levels were 1.2 and 2.5 fold higher in PHD2 haplodeficient macrophages, and 1.3 and 12.2 fold higher in PHD2 null macrophages (Supplementary Figure 7). PHD3 silencing induced NF-κB activity by 22% and 14% in $PHD2^{LysCre;wt/wt}$ and $PHD2^{LysCre;lox/wt}$ macrophages but by 70% in $PHD2^{LysCre;lox/lox}$ macrophages compared to their scramble controls (Figure 6G and Supplementary Note 4). These data indicate that PHD3 induction in PHD2 null macrophages is responsible for the repression of NF-κB activity. This may explain, at least in part, the absence of enhanced collateral growth and ischemic protection in mice lacking two PHD2 alleles in myeloid cells.

To understand if hydroxylase function was necessary for PHD2 mediated NF-kB regulation, $PHD2^{+/-}$ macrophages were electroporated with a plasmid carrying a wild type PHD2 ($PHD2^{wt}$) or a hydroxylase-deficient PHD2 containing a mutation in a critical residue of the catalytic site ($PHD2^{H313A}$)[50]. Ectopic expression of $PHD2^{wt}$ greatly blunted the activity of NF-κB luciferase induced by PHD2 haplodeficiency, whereas $PHD2^{H313A}$ had no effect (Figure 6H), suggesting a functional role of PHD2 hydroxylase activity in the downregulation of NF-κB pathway. We also assessed the effect of TNF-α, archetypal

cytokine activating the canonical NF-κB pathway[18], in WT and PHD2$^{+/-}$ macrophages and found that TNF-α-induced NF-κB activation was significantly stronger in PHD2 haplodeficient macrophages (Figure 6I). In contrast, basal and TNF-α-induced NF-κB activity were comparable in WT and PHD2$^{+/-}$ ECs (Supplementary Figure 8A). When measuring the nuclear accumulation of NF-κB subunits, we found that the members of the canonical pathway p65 (RelA) and p50 (NF-κB1) were more abundant in PHD2$^{+/-}$ than WT macrophages (Figure 6J). Silencing of p65 or p50 blocked NF-κB hyperactivation in PHD2$^{+/-}$ macrophages and the combined knockdown of both subunits restored NF-κB function back to the WT levels (Figure 6K and Supplementary Note 5), thus highlighting the prominent role of NF-κB p65/p50 heterodimers in macrophages.

To evaluate the involvement of the canonical NF-κB signaling in macrophage skewing by PHD2 haplodeficiency, we generated a myeloid specific double transgenic strain, heterozygous deficient for PHD2 and null for IKKβ, a positive regulator of NF-κB canonical pathway. Disruption of NF-κB canonical pathway via genetic deletion of IKKβ prevented the upregulation of Tie2, PDGFB and SDF1 in cultured PHD2 haplodeficient macrophages (Figure 6L). Similar results were obtained by treating macrophages with the NF-κB inhibitor 6-amino-4-(4-phenoxyphenylethylamino)quinazoline (Supplementary Figure 8B). In vivo, genetic inactivation of IKKβ in myeloid cells abolished the enhanced production of circulating TEMs (Figure 6M) and collateral vessel preconditioning induced by myeloid PHD2 haplodeficiency (Figure 6N). Remarkably, myeloid specific IKKβ gene targeting in WT mice greatly prevented ischemia-induced arteriogenesis, occuring 7 days post-ligation (Figure 6N).

Thus, skewing of PHD2 haplodeficient macrophages towards an arteriogenic phenotype relies on the activation of the NF-κB canonical pathway.

DISCUSSION

Specific macrophage subsets / differentiation states have been implicated in the promotion of angiogenesis during cancer and atherosclerosis progression[11,12]. However, little is known of the significance of macrophage heterogeneity in arteriogenesis and its implications on ischemic diseases. This study identifies a role of myeloid PHD2 in oxygen delivery by regulating arteriogenesis. Reduced PHD2 levels in macrophages determine a specific gene signature that fosters the arteriogenic program by inducing recruitment and growth of SMCs. This program relies on NF-κB-dependent upregulation of macrophage-derived SDF1, PDGFB, and the angiopoietin receptor, Tie2. We show that the phenotype of macrophages induced by reduced levels of myeloid PHD2 not only favors the formation of new collateral branches, but is also important for collateral vessel homeostasis. Under steady-state conditions, blood monocytes act as circulating precursors that migrate into non-inflamed tissue to replace certain subsets of tissue macrophages[51]. PHD2 haplodeficient bone marrows in WT recipient mice enhanced collateral formation already at baseline ("collateral vessel preconditioning"). However, when $PHD2^{+/-}$ mice were transplanted with a WT bone marrow, preexisting collaterals regressed to the same level as in WT mice, suggesting a role of tissue macrophages in sustaining artery maintenance. The proarteriogenic tissue macrophages identified in the present study are reminiscent of the M2-like, proangiogenic macrophage subset, known as TEMs, which are found in tumors and developing or regenerating tissues[29-31,49]. The macrophages here described do not upregulate either VEGF or inflammatory genes, but express increased levels of Tie2, Nrp1, CXCR4, PDGFB and SDF1. Unlike tumor-associated TEMs, the cells described here express high levels of the MCP1 receptor, CCR2. Tissue- and tumor-infiltrating TEMs appear to originate from a distinct subset of circulating Tie2-expressing monocytes (our data and [29]). In agreement with previous studies[49], Tie2-expressing monocytes as well as Tie2-expressing macrophages were scarce in the peripheral blood and adductor of WT mice, but were abundant in PHD2 haplodeficient mice in resting conditions or in the pericollaterel region of WT mice after occlusion of the major arterial route. Their depletion abrogated the arterial vessel preconditioning in $PHD2^{+/-}$ mice and prevented ischemia-induced arteriogenesis in WT mice, supporting the role of TEMs in blood flow recovery during occlusive diseases. The model we propose is described in Supplementary Figure 9.

After femoral artery ligation, a surge of chemoattractants recruits TEMs from the blood to the pericollateral region. Here, TEMs fuel the tissue with SDF1 and PDGFB. The combined activity of these two cytokines will induce SMC migration, positioning, dedifferentiation, and growth, altogether resulting in artery maturation. PHD2 haplodeficiency unleashes constitutive NF-κB signals that result in a larger reservoir of circulating and tissue-resident TEMs. Production of SDF1 and PDGFB by TEMs accounts for the enhanced arteriogenesis at baseline and thus protection against ischemic tissue demise. It remains an open question by which mechanism PHD2 activity / levels are reduced in WT mononuclear phagocytes. In general, PHD2 needs oxygen as cosubstrate and partly loses its activity under hypoxia. Furthermore, cytokine-driven downregulation of PHD2 expression will also result in reduced enzymatic activity independent of oxygen availability[52,53]. Here, we show that PHD2 hydroxylase function (and thus oxygen) is required to repress NF-κB and that PHD2 levels are decreased in tissue macrophages after ischemia. Thus, there might be two potentially different levels of regulation of monocyte/macrophage polarization by PHD2. The first might occur in the bone marrow where mean oxygen tension is normally 50 mmHg (ca. 7%)[54]. At this oxygen tension, PHD2 activity will be partly inhibited in WT macrophages, to a similar extent as it occurs in $PHD2^{+/-}$ macrophages[25,55-57]. After femoral artery occlusion, the bulk of blood flow is redirected into collateral conduits, generating shear stress that causes the release of different cytokines by the endothelium. Collateral formation is recognized as a hypoxia-independent process[13, 14]. Nevertheless, stimulation by these cytokines might explain the transcriptional repression of PHD2 measured in infiltrating WT macrophages (but not in $PHD2^{+/-}$ macrophages that constitutively express half levels of PHD2) and thus strengthen their arteriogenic response. Noteworthy, separate studies have reported that angiopoietin(s) as well as TGFß reduce PHD2 expression ([52,53] and M.M., unpublished), and enhance collateral vascularization, in part through a direct effect on monocytes/macrophages[58-61]. Overall, genetic deletion of one PHD2 allele preadapts macrophages to ischemia and causes polarization towards an arteriogenic phenotype.

Genetic studies in mice on macrophage-associated cytokine receptors, or on cytokines, have elucidated the importance of specific biological axes such as SDF1/CXCR4, MCP1/CCR2, VEGF/Nrp1 and others, in arteriogenesis and post-ischemic revascularization[6, 32-36, 62-66]. The population of macrophages described in the current

manuscript is enriched in Tie2, CXCR4, CCR2, and Nrp1 expression. By using Tie2 as a marker to identify (and to deplete) a subset of monocytes/macrophages, we define for the first time the role of PHD2 in macrophage skewing and unravel a new mechanism whereby an oxygen sensor leads to blood recovery through collateral arteriogenesis, fostered by M2-like macrophages. Further investigations will be needed to understand if this model plays a role during developmental arteriogenesis, if the Tie2-expressing population here described is similar to the one found in cancer, and if Tie2 expressed by these cells has a functional role as in tumor-associated TEMs[29-31]. Recently, TEM-like embryonic macrophages have been found to be involved in anastomosis of vessels during development[46]. Given the fact that collateral vessels in the limb grow and mature from preexisting anastomoses[6], we cannot exclude that enhanced collateralization in PHD2$^{+/-}$ mice is, at least in part, due to this process as well. Nevertheless, acute deletion of one PHD2 allele in macrophages leads to almost complete protection against ischemic necrosis by induction of arterial collateral branches, thus supporting the idea that enhanced arteriogenesis by PHD2 haplodeficiency can promptly occur in adults.

Although different proarteriogenic molecules such as MMP2 are upregulated in PHD2$^{+/-}$ macrophages, SDF1 and PDGFB were expressed more abundantly. Both cytokines are potent chemoattractants for SMCs and/or SMC progenitors[41-43]. SDF1 more specifically plays a key-role in recruiting, retaining and positioning CXCR4^{+} cells[67,68]. This might be the case for SMCs and SMC progenitors, both positive for the SDF1 receptor CXCR4[41,69], which can find their way towards collaterals by following a gradient of SDF1 released by pericollateral TEMs. PDGFB sustains recruitment and proliferation of SMCs and SMC progenitors at the site of expression[42]. In our experiments, combined activation of SDF1 and PDGFB results in the complete formation of collateral branches, suggesting that in SMCs, these two pathways can converge to, at least in part, overlapping downstream effectors. An open question is to understand whether, in PHD2$^{+/-}$ monocytes/macrophages, the release of SDF1 and PDGFB are directly downstream of the NF-κB pathway or are consequent to Tie2 signaling activation[29].

TEMs are a subpopulation of alternatively activated (M2) macrophages. We show here that macrophage skewing by PHD2 haplodeficiency is driven by the canonical NF-κB pathway. The NF-κB family consists of 5 members: NF-κB1 (p105/p50), NF-κB2 (p100/p52), RelA (p65), RelB, and c-Rel[18,70,71], which may form different homo- and

heterodimers associated with differential regulation of target genes. Activation of NF-κB typically involves phosphorylation-dependent degradation of IκB inhibitors by the IκB kinase (IKK) complex. This releases NF-κB and allows it to translocate freely to the nucleus. HIF-prolyl hydroxylases are repressors of NF-κB activity, likely via their potential to directly hydroxylate IKKβ[20,21]. Alternatively, PHD3 has been also shown to associate with IKKβ independently of its hydroxylase function, thereby blocking further interaction between IKKβ and the chaperone Hsp90, which is required for IKKβ phosphorylation and release of NF-κB[19]. Thus, the hydroxylase function of PHD oxygen sensors can be either necessary or dispensable for the downregulation of NF-κB depending on the cellular context (our data and [15]). By different means, we prove that PHD2 haplodeficiency results in the hyperactivation of the canonical NF-κB pathway in macrophages via accumulation of p65 and p50 subunits. Genetic or pharmacological inhibition of the NF-κB pathway prevents the upregulation of Tie2, PDGFB, and SDF1 in cultured PHD2 haplodeficient macrophages. In vivo, genetic inactivation of myeloid IKKβ inhibits TEM production and collateral vessel preconditioning induced by PHD2 haplodeficiency. Previous evidence has shown that IKKβ suppresses the M1 phenotype and promotes M2 macrophage skewing through positive regulation of the canonical NF-κB pathway[72-74]. From a molecular point of view, the main downstream effectors of the canonical NF-κB pathway are p65 and p50, existing mostly as heterodimers. Homodimers of the p50 subunit of NF-κB, which lack transactivation domains, can repress expression of NF-κB target genes and inhibit inflammation, whereas the homodimers of p65 as well as the p65/p50 heterodimers are responsible for NF-κB-mediated gene transcription[18,70,71]. Consistent with a role of PHD oxygen sensors in the negative regulation of IKKβ, we show that PHD2 haplodeficiency triggers p65 and p50 accumulation and thus leads to the repression of M1 genes and reinforcement of M2 genes. This is in line with the above-cited literature showing repression of M2-markers and increased expression of M1-markers in IKKβ deficient macrophages[72-74]. Another study shows that deficiency, not accumulation, of p50 in bone marrow cells prompts macrophage infiltration and elicits arteriogenesis[75]. At first glance, this might appear in conflict with our findings. Nevertheless, the same study reports that p50 ablation favors a (compensatory) p65 accumulation. Thus, both the elimination of negative (p50-mediated) NF-κB breaking cues and endorsement of the (p65-mediated)

NF-κB transactivating potential will tilt the balance towards a positive regulation of the NF-κB canonical pathway and enhanced macrophage-initiated arteriogenesis. Interestingly, complete deletion of PHD2 in macrophages elicits a potent induction of PHD3 levels that compensate for the absence of PHD2 and thus reestablish the activity of NF-κB to the WT levels. In contrast, a mild induction of PHD3 in PHD2 haplodeficient macrophages does not counterbalance the positive effect of PHD2 downmodulation on NF-κB pathway. Therefore, consistent with previous findings[76], feedback loops involving PHD3 oxygen sensor tune the genetic program triggered by PHD2 inactivation. As a consequence, heterozygous but not homozygous inactivation of PHD2 is able to mount a safety program in myeloid cells through NF-κB activation that enhances collateralization and thus prevents ischemic necrosis.

In our previous work, we show that deficiency or inhibition of the oxygen sensor PHD1, belonging to the same family as PHD2, induces hypoxia tolerance by reprogramming basal metabolism towards glycolysis, that allows anaerobic ATP production in ischemia[77]. This phenotype was specific for $PHD1^{-/-}$ mice but not for $PHD2^{+/-}$ and $PHD3^{-/-}$ mice[77]. However, while the previous investigation was carried out in a mixed background (Swiss/129), the current study was performed in a BalbC and 129S6 background. It is known that strain-related genetic differences profoundly affect the formation of collateral vasculature and thus the outcome of ischemia after femoral artery ligation[78]. Indeed, collateral formation in $PHD2^{+/-}$ mice and ischemic necrosis in a Swiss/129 background were comparable to their littermate controls (data not shown). Also, in any of the $PHD2^{+/-}$ strains analyzed, the levels of the peroxisome proliferator-activated receptor α (PPARα) and the pyruvate dehydrogenase kinases PDK1 and PDK4 (induced in $PHD1^{-/-}$ fibers and driving the metabolic reprogramming at baseline) were not affected[77], supporting a different mechanism of protection against ischemia in $PHD2^{+/-}$ mice.

Finally, our findings have potential medical implications. Previous studies have shown that unspecific inhibitors of PHD2 or silencing of PHD2 promotes therapeutic revascularization against ischemia[16,22-24]. However, this approach can have some limitations. First, angiogenesis is a late response; therefore, organ function might be compromised until new vessel formation is complete. In contrast, arteriogenesis takes place on preexisting vascular shunts and this process is actually the first to be triggered in

case of ischemia[6]. Second, the generation of PHD2-specific inhibitors will be challenging due to the high homology of the catalytic pocket of the three PHD family members (PHD1, PHD2 and PHD3)[17]. Overall, a cell-based therapy with PHD2 hypomorphic macrophages or Tie2-expressing macrophages might promote collateral vascularization in patients at risk of ischemic damage, i.e. diabetic or hypercholesterolemic patients[79]; similar results may be obtained by combined administration of SDF1 and PDGFB. At this stage, our study provides insight into how PHD2 oxygen sensor regulates arteriogenesis via controlling a specific monocyte / macrophage phenotype and thus guarantees oxygen delivery in case of shortage, as it occurs during ischemia.

METHODS SUMMARY

129/S6 or Balb/C WT and PHD2$^{+/-}$ mice (8-12 weeks old) were obtained from our mouse facility. PHD2$^{+/-}$ and PHD2 conditional knockout mice were obtained as previously described[25]. To induce hind limb ischemia, unilateral or bilateral ligations of the femoral artery and vein and the cutaneous vessels branching from the caudal femoral artery side branch were performed without damaging the nervus femoralis[80]. Oxgen tension (pO_2) in the lower limb was measured 12 hours after femoral artery ligation by using ^{19}F-MRI oximetry. Adductor crural muscles were dissected, fixed in 2% PFA, dehydrated, embedded in paraffin and sectioned at 7μm thickness for histology, immunostaining and morphometry analysis. Macrophages were either harvested from the peritoneal cavity of the mice (peritoneal macrophages (pMØ)) or derived from bone marrow precursors as described before[81]. Balb/c WT and PHD2$^{+/-}$ recipient mice were irradiated with 7.5 Gy. Subsequently, 5x10^6 bone marrow cells from green fluorescent protein$^+$ (GFP$^+$) WT or GFP$^+$ PHD2$^{+/-}$ mice were injected intravenously via the tail vein. Femoral artery ligation, treadmill running test and bismuth angiography were performed 6 weeks after bone marrow reconstitution. Full Methods and any associated references are available in the Supplementary Information.

REFERENCES

1. Carmeliet, P. Mechanisms of angiogenesis and arteriogenesis. *Nat Med* **6**, 389-95 (2000).

2. Schirmer, S.H., van Nooijen, F.C., Piek, J.J. & van Royen, N. Stimulation of collateral artery growth: travelling further down the road to clinical application. *Heart* **95**, 191-7 (2009).

3. Simons, M. & Ware, J.A. Therapeutic angiogenesis in cardiovascular disease. *Nat Rev Drug Discov* **2**, 863-71 (2003).

4. Yu, J. et al. Endothelial nitric oxide synthase is critical for ischemic remodeling, mural cell recruitment, and blood flow reserve. *Proc Natl Acad Sci U S A* **102**, 10999-1004 (2005).

5. Schultz, A. et al. Interindividual heterogeneity in the hypoxic regulation of VEGF: significance for the development of the coronary artery collateral circulation. *Circulation* **100**, 547-52 (1999).

6. Schaper, W. Collateral circulation: past and present. *Basic Res Cardiol* **104**, 5-21 (2009).

7. van Royen, N. et al. Effects of local MCP-1 protein therapy on the development of the collateral circulation and atherosclerosis in Watanabe hyperlipidemic rabbits. *Cardiovasc Res* **57**, 178-85 (2003).

8. Heil, M. & Schaper, W. Influence of mechanical, cellular, and molecular factors on collateral artery growth (arteriogenesis). *Circ Res* **95**, 449-58 (2004).

9. Heil, M. et al. Blood monocyte concentration is critical for enhancement of collateral artery growth. *Am J Physiol Heart Circ Physiol* **283**, H2411-9 (2002).

10. Ito, W.D. et al. Monocyte chemotactic protein-1 increases collateral and peripheral conductance after femoral artery occlusion. *Circ Res* **80**, 829-37 (1997).

11. Mantovani, A. & Sica, A. Macrophages, innate immunity and cancer: balance, tolerance, and diversity. *Curr Opin Immunol* **22**, 231-7.

12. Mantovani, A., Garlanda, C. & Locati, M. Macrophage diversity and polarization in atherosclerosis: a question of balance. *Arterioscler Thromb Vasc Biol* **29**, 1419-23 (2009).

13. Ito, W.D. et al. Angiogenesis but not collateral growth is associated with ischemia after femoral artery occlusion. *Am J Physiol* **273**, H1255-65 (1997).

14. Gray, C. et al. Ischemia is not required for arteriogenesis in zebrafish embryos. *Arterioscler Thromb Vasc Biol* **27**, 2135-41 (2007).

15. Chan, D.A. et al. Tumor vasculature is regulated by PHD2-mediated angiogenesis and bone marrow-derived cell recruitment. *Cancer Cell* **15**, 527-38 (2009).

16. Loinard, C. et al. Inhibition of prolyl hydroxylase domain proteins promotes therapeutic revascularization. *Circulation* **120**, 50-9 (2009).

17. Fraisl, P., Aragones, J. & Carmeliet, P. Inhibition of oxygen sensors as a therapeutic strategy for ischaemic and inflammatory disease. *Nat Rev Drug Discov* **8**, 139-52 (2009).

18. Lawrence, T. The nuclear factor NF-kappaB pathway in inflammation. *Cold Spring Harb Perspect Biol* **1**, a001651 (2009).

19. Xue, J. et al. Prolyl hydroxylase-3 is down-regulated in colorectal cancer cells and inhibits IKKbeta independent of hydroxylase activity. *Gastroenterology* **138**, 606-15.

20. Cummins, E.P. et al. Prolyl hydroxylase-1 negatively regulates IkappaB kinase-beta, giving insight into hypoxia-induced NFkappaB activity. *Proc Natl Acad Sci U S A* **103**, 18154-9 (2006).

21. Fu, J. & Taubman, M.B. Prolyl hydroxylase EGLN3 regulates skeletal myoblast differentiation through an NF-kappaB-dependent pathway. *J Biol Chem* **285**, 8927-35.

22. Milkiewicz, M., Pugh, C.W. & Egginton, S. Inhibition of endogenous HIF inactivation induces angiogenesis in ischaemic skeletal muscles of mice. *J Physiol* **560**, 21-6 (2004).

23. Nangaku, M. et al. A novel class of prolyl hydroxylase inhibitors induces angiogenesis and exerts organ protection against ischemia. *Arterioscler Thromb Vasc Biol* **27**, 2548-54 (2007).

24. Huang, M. et al. Short hairpin RNA interference therapy for ischemic heart disease. *Circulation* **118**, S226-33 (2008).

25. Mazzone, M. et al. Heterozygous deficiency of PHD2 restores tumor oxygenation and inhibits metastasis via endothelial normalization. *Cell* **136**, 839-51 (2009).

26. Aranguren, X.L. et al. MAPC transplantation confers a more durable benefit than AC133+ cell transplantation. *Cell Transplant*.

27. Pugh, C.W. & Ratcliffe, P.J. Regulation of angiogenesis by hypoxia: role of the HIF system. *Nat Med* **9**, 677-84 (2003).

28. Patel, T.H., Kimura, H., Weiss, C.R., Semenza, G.L. & Hofmann, L.V. Constitutively active HIF-1alpha improves perfusion and arterial remodeling in an endovascular model of limb ischemia. *Cardiovasc Res* **68**, 144-54 (2005).

29. Pucci, F. et al. A distinguishing gene signature shared by tumor-infiltrating Tie2-expressing monocytes, blood "resident" monocytes, and embryonic macrophages suggests common functions and developmental relationships. *Blood* **114**, 901-14 (2009).

30. De Palma, M. et al. Tie2 identifies a hematopoietic lineage of proangiogenic monocytes required for tumor vessel formation and a mesenchymal population of pericyte progenitors. *Cancer Cell* **8**, 211-26 (2005).

31. Mazzieri, R. et al. Targeting the ANG2/TIE2 Axis Inhibits Tumor Growth and Metastasis by Impairing Angiogenesis and Disabling Rebounds of Proangiogenic Myeloid Cells. *Cancer Cell* **19**, 512-26.

32. Nickerson, M.M. et al. Bone marrow-derived cell-specific chemokine (C-C motif) receptor-2 expression is required for arteriolar remodeling. *Arterioscler Thromb Vasc Biol* **29**, 1794-801 (2009).

33. Cochain, C. et al. Regulation of monocyte subset systemic levels by distinct chemokine receptors controls post-ischaemic neovascularization. *Cardiovasc Res* **88**, 186-95.

34. Heil, M. et al. Collateral artery growth (arteriogenesis) after experimental arterial occlusion is impaired in mice lacking CC-chemokine receptor-2. *Circ Res* **94**, 671-7 (2004).

35. Fujii, T. et al. Nonendothelial mesenchymal cell-derived MCP-1 is required for FGF-2-mediated therapeutic neovascularization: critical role of the inflammatory/arteriogenic pathway. *Arterioscler Thromb Vasc Biol* **26**, 2483-9 (2006).

36. Zacchigna, S. et al. Bone marrow cells recruited through the neuropilin-1 receptor promote arterial formation at the sites of adult neoangiogenesis in mice. *J Clin Invest* **118**, 2062-75 (2008).

37. Qian, B.Z. & Pollard, J.W. Macrophage diversity enhances tumor progression and metastasis. *Cell* **141**, 39-51.

38. Clausen, B.E., Burkhardt, C., Reith, W., Renkawitz, R. & Forster, I. Conditional gene targeting in macrophages and granulocytes using LysMcre mice. *Transgenic Res* **8**, 265-77 (1999).

39. Takeda, K. et al. Placental but not heart defects are associated with elevated hypoxia-inducible factor alpha levels in mice lacking prolyl hydroxylase domain protein 2. *Mol Cell Biol* **26**, 8336-46 (2006).

40. El Kasmi, K.C. et al. Toll-like receptor-induced arginase 1 in macrophages thwarts effective immunity against intracellular pathogens. *Nat Immunol* **9**, 1399-406 (2008).

41. Karshovska, E., Zagorac, D., Zernecke, A., Weber, C. & Schober, A. A small molecule CXCR4 antagonist inhibits neointima formation and smooth muscle progenitor cell mobilization after arterial injury. *J Thromb Haemost* **6**, 1812-5 (2008).

42. Hellstrom, M., Kalen, M., Lindahl, P., Abramsson, A. & Betsholtz, C. Role of PDGF-B and PDGFR-beta in recruitment of vascular smooth muscle cells and pericytes during embryonic blood vessel formation in the mouse. *Development* **126**, 3047-55 (1999).

43. Cao, R. et al. Angiogenic synergism, vascular stability and improvement of hind-limb ischemia by a combination of PDGF-BB and FGF-2. *Nat Med* **9**, 604-13 (2003).

44. Wolf, C. et al. Vascular remodeling and altered protein expression during growth of coronary collateral arteries. *J Mol Cell Cardiol* **30**, 2291-305 (1998).

45. Kumar, M.S. & Owens, G.K. Combinatorial control of smooth muscle-specific gene expression. *Arterioscler Thromb Vasc Biol* **23**, 737-47 (2003).

46. Fantin, A. et al. Tissue macrophages act as cellular chaperones for vascular anastomosis downstream of VEGF-mediated endothelial tip cell induction. *Blood*.

47. Sunderkotter, C. et al. Subpopulations of mouse blood monocytes differ in maturation stage and inflammatory response. *J Immunol* **172**, 4410-7 (2004).

48. Geissmann, F. et al. Blood monocytes: distinct subsets, how they relate to dendritic cells, and their possible roles in the regulation of T-cell responses. *Immunol Cell Biol* **86**, 398-408 (2008).

49. De Palma, M., Venneri, M.A., Roca, C. & Naldini, L. Targeting exogenous genes to tumor angiogenesis by transplantation of genetically modified hematopoietic stem cells. *Nat Med* **9**, 789-95 (2003).

50. Jokilehto, T. et al. Retention of prolyl hydroxylase PHD2 in the cytoplasm prevents PHD2-induced anchorage-independent carcinoma cell growth. *Exp Cell Res* **316**, 1169-78.

51. Geissmann, F., Jung, S. & Littman, D.R. Blood monocytes consist of two principal subsets with distinct migratory properties. *Immunity* **19**, 71-82 (2003).

52. Chen, J.X. & Stinnett, A. Ang-1 gene therapy inhibits hypoxia-inducible factor-1alpha (HIF-1alpha)-prolyl-4-hydroxylase-2, stabilizes HIF-1alpha expression, and normalizes immature vasculature in db/db mice. *Diabetes* **57**, 3335-43 (2008).

53. McMahon, S., Charbonneau, M., Grandmont, S., Richard, D.E. & Dubois, C.M. Transforming growth factor beta1 induces hypoxia-inducible factor-1 stabilization through selective inhibition of PHD2 expression. *J Biol Chem* **281**, 24171-81 (2006).

54. Harrison, J.S., Rameshwar, P., Chang, V. & Bandari, P. Oxygen saturation in the bone marrow of healthy volunteers. *Blood* **99**, 394 (2002).

55. Chan, D.A., Sutphin, P.D., Yen, S.E. & Giaccia, A.J. Coordinate regulation of the oxygen-dependent degradation domains of hypoxia-inducible factor 1 alpha. *Mol Cell Biol* **25**, 6415-26 (2005).

56. Pan, Y. et al. Multiple factors affecting cellular redox status and energy metabolism modulate hypoxia-inducible factor prolyl hydroxylase activity in vivo and in vitro. *Mol Cell Biol* **27**, 912-25 (2007).

57. Epstein, A.C. et al. C. elegans EGL-9 and mammalian homologs define a family of dioxygenases that regulate HIF by prolyl hydroxylation. *Cell* **107**, 43-54 (2001).

58. van Royen, N. et al. Exogenous application of transforming growth factor beta 1 stimulates arteriogenesis in the peripheral circulation. *FASEB J* **16**, 432-4 (2002).

59. Kobayashi, K. et al. Combination of in vivo angiopoietin-1 gene transfer and autologous bone marrow cell implantation for functional therapeutic angiogenesis. *Arterioscler Thromb Vasc Biol* **26**, 1465-72 (2006).

60. Shyu, K.G., Manor, O., Magner, M., Yancopoulos, G.D. & Isner, J.M. Direct intramuscular injection of plasmid DNA encoding angiopoietin-1 but not angiopoietin-2 augments revascularization in the rabbit ischemic hindlimb. *Circulation* **98**, 2081-7 (1998).

61. Tressel, S.L. et al. Angiopoietin-2 stimulates blood flow recovery after femoral artery occlusion by inducing inflammation and arteriogenesis. *Arterioscler Thromb Vasc Biol* **28**, 1989-95 (2008).

62. Zhou, J. et al. CXCR3-dependent accumulation and activation of perivascular macrophages is necessary for homeostatic arterial remodeling to hemodynamic stresses. *J Exp Med* **207**, 1951-66.

63. Jin, D.K. et al. Cytokine-mediated deployment of SDF-1 induces revascularization through recruitment of CXCR4+ hemangiocytes. *Nat Med* **12**, 557-67 (2006).

64. Seeger, F.H. et al. CXCR4 expression determines functional activity of bone marrow-derived mononuclear cells for therapeutic neovascularization in acute ischemia. *Arterioscler Thromb Vasc Biol* **29**, 1802-9 (2009).

65. Yla-Herttuala, S. & Alitalo, K. Gene transfer as a tool to induce therapeutic vascular growth. *Nat Med* **9**, 694-701 (2003).

66. Seiler, C. et al. Promotion of collateral growth by granulocyte-macrophage colony-stimulating factor in patients with coronary artery disease: a randomized, double-blind, placebo-controlled study. *Circulation* **104**, 2012-7 (2001).

67. Grunewald, M. et al. VEGF-induced adult neovascularization: recruitment, retention, and role of accessory cells. *Cell* **124**, 175-89 (2006).

68. Bagri, A. et al. The chemokine SDF1 regulates migration of dentate granule cells. *Development* **129**, 4249-60 (2002).

69. Zernecke, A. et al. SDF-1alpha/CXCR4 axis is instrumental in neointimal hyperplasia and recruitment of smooth muscle progenitor cells. *Circ Res* **96**, 784-91 (2005).

70. Li, Q. & Verma, I.M. NF-kappaB regulation in the immune system. *Nat Rev Immunol* **2**, 725-34 (2002).

71. Perkins, N.D. Integrating cell-signalling pathways with NF-kappaB and IKK function. *Nat Rev Mol Cell Biol* **8**, 49-62 (2007).

72. Fong, C.H. et al. An antiinflammatory role for IKKbeta through the inhibition of "classical" macrophage activation. *J Exp Med* **205**, 1269-76 (2008).

73. Hagemann, T. et al. "Re-educating" tumor-associated macrophages by targeting NF-kappaB. *J Exp Med* **205**, 1261-8 (2008).

74. Greten, F.R. et al. NF-kappaB is a negative regulator of IL-1beta secretion as revealed by genetic and pharmacological inhibition of IKKbeta. *Cell* **130**, 918-31 (2007).

75. de Groot, D., Haverslag, R.T., Pasterkamp, G., de Kleijn, D.P. & Hoefer, I.E. Targeted deletion of the inhibitory NF-kappaB p50 subunit in bone marrow-derived cells improves collateral growth after arterial occlusion. *Cardiovasc Res* **88**, 179-85.

76. Moslehi, J. et al. Loss of Hypoxia-Inducible Factor Prolyl Hydroxylase Activity in Cardiomyocytes Phenocopies Ischemic Cardiomyopathy. *Circulation* (2010).

77. Aragones, J. et al. Deficiency or inhibition of oxygen sensor Phd1 induces hypoxia tolerance by reprogramming basal metabolism. *Nat Genet* **40**, 170-80 (2008).

78. Helisch, A. et al. Impact of mouse strain differences in innate hindlimb collateral vasculature. *Arterioscler Thromb Vasc Biol* **26**, 520-6 (2006).

79. Sacco, R.L. Risk factors and outcomes for ischemic stroke. *Neurology* **45**, S10-4 (1995).

80. Luttun A, T.M., Moons L, Wu Y, Angelillo-Scherrer A, Liao F, Nagy JA, Hooper A, Priller J, De Klerck B, Compernolle V, Daci E, Bohlen P, Dewerchin M, Herbert JM, Fava R, Matthys P, Carmeliet G, Collen D, Dvorak HF, Hicklin DJ, Carmeliet P. Revascularization of ischemic tissues by PlGF treatment, and inhibition of tumor angiogenesis, arthritis and atherosclerosis by anti-Flt1. *Nat Med* **8**, 831-840 (2002).

81. Meerpohl, H.G., Lohmann-Matthes, M.L. & Fischer, H. Studies on the activation of mouse bone marrow-derived macrophages by the macrophage cytotoxicity factor (MCF). *Eur J Immunol* **6**, 213-7 (1976).

SUPPLEMENTARY INFORMATION (SI)

Supplementary Information is linked to the main manuscript.

A figure (Supplementary Figure 9) summarizing the main result of this paper is also included as SI.

ACKNOWLEDGEMENTS

The authors thank Y. Jonsson, T. Janssens, A. Bouché, A. Carton, A. Manderveld, B. Vanwetswinkel and N. Dai for technical assistance. This work was supported by grants from FWO (G.0726.10), Belgium, and from VIB. The authors are thankful to Dr. P. Carmeliet for scientific discussion and support. VE-Cadherin:CreERT and PDGFRB:Cre transgenic mice were generated at the Cancer Research UK (London, UK) and kindly donated by Dr. R. Adams. The IKKβ floxed mice are a generous gift of Dr. M. Karin (UCSD, La Jolla, CA). The hydroxylase-deficient PHD2 construct was given by Dr. P. Ratcliffe (Oxford, UK). ED was granted by ARC, SC by FCT, RLO and VF by FWO, AH by DFG. CR was supported by COST action TD0901. MDP was supported by an ERC starting grant.

AUTHOR INFORMATION

AFFILIATIONS

Vesalius Research Center, VIB, KUL, Leuven, Belgium
Y. Takeda, S. Costa, E. Delamarre, C. Roncal, R. Leite De Oliveira, V. Finisguerra, P. F. Bruyère, S. Deschoemaeker, M. Wenes, A. Hamm, J. Serneels & M. Mazzone

Life and Health Sciences Research Institute, Minho University, Braga, Portugal
S. Costa

Atherosclerosis Research Laboratory, CIMA-University of Navarra, Pamplona, Spain
C. Roncal

Angiogenesis and Tumor Targeting Unit, HSR-TIGET and Vita-Salute University, San Raffaele Institute, Milan, Italy
M.L. Squadrito & M. De Palma

Biomedical Magnetic Resonance Unit, Medicinal Chemistry and Radiopharmacy U.C.Louvain, Brussels, Belgium
J. Magat, B.F. Jordan & B. Gallez

Rayne Institute, University College London, London, UK

T. Bhattacharrya & Patrick Maxwell

Cardiovascular Medicine, Yale University, New Haven, CT, USA
Z. Zhuang & M. Simons

Molecular/Cancer Biology Laboratory, Research Programs Unit, Institute for Molecular Medicine, Helsinki, Finland
A. Anisimov & K. Alitalo

The First Department of Internal Medicine, Nara Medical University, Nara, Japan
Y. Saito

CONTRIBUTIONS

Y.T., E.D. and S.C. performed experimental design, all experiments, acquisition of data and analysis and interpretation of all data. C.R. performed analysis of histological stainings, angiographies. R.L.O., C.R and S.C. performed the western blots. R.L.O and V.F performed treadmill-running tests, RT-PCR experiments and drug administrations. M.L.S. performed bone marrow derived, lineage negative hematopoietic cells isolation and transduction and vector copy number analysis. F.B. performed EC isolation and angiography measurements. J.M., B.F.J. and B.G. performed oxymetry experiments. S.D. performed luciferase assays and management of the colonies. M.W. and A.H performed transplantation experiments and electroporations. Y.T. and J.S. performed the ligations of the femoral artery. Z.Z and M.S. performed micro-CT angiograms. A.A. and K.A. have contributed with viral vector productions. T.B. and P.M. contributed to the generation of the PHD2 targeting vector. Y.T., E.D., S.C., C.R., Y.S. and M.D.P. participated in scientific discussion and drafting of the manuscript. M.M. performed experimental design, analysis of data, conducted scientific direction, wrote manuscript.

COMPETING FINANCIAL INTERESTS

No competing financial interests to declare.

CORRESPONDING AUTHOR

Correspondence to: M. Mazzone (massimiliano.mazzone@vib-kuleuven.be)

FIGURE LEGENDS

FIGURE 1: PHD2 HAPLODEFICIENCY ENHANCES PERFUSION AND REDUCES ISCHEMIC DAMAGE

A, $PHD2^{+/-}$ mice present increased toe perfusion (laser Doppler analysis) at 12, 24 and 48 hours after femoral artery ligation compared to WT mice (N=7-13; P<0.05). **B,** Partial loss of PHD2 improves functional endurance (treadmill running test) 12 hours after ligation, despite comparable performance at baseline (N=5; P<0.05). **C,D,** Micrographs of the MRI-based oxymetry revealing increased oxygenation of the crural muscle in $PHD2^{+/-}$ mice (D) versus WT controls (C) 12 hours after ligation. **E,** Quantification of the MRI-based oxymetry represented in C,D (N=5; P=0.02). **F-I,** Staining for pimonidazole on cross-sections through the crural muscle at baseline (F,G) and 12 hours after femoral artery ligation (H,I) in WT and $PHD2^{+/-}$ mice. **J,** Pimonidazole positive area is significantly reduced in $PHD2^{+/-}$ compared to WT mice 12 hours after ligation (N=4; P=0.03). **K,L,** H&E staining illustrating reduced necrotic area in $PHD2^{+/-}$ soleus (as part of the crural muscle) (L) versus WT soleus (K) 72 hours after femoral artery ligation. **M,** Quantification of the necrotic area represented in K,L (N=8; P=0.002). **N,O,** Crural muscle viability by 2,3,5-triphenyltetrazolium chloride (TTC) staining is increased in $PHD2^{+/-}$ mice (O) 72 hours after ischemia. **P,** Quantification of the TTC staining represented in N,O (N=8; P=0.0002). **Q,R** Cross-sections through the heart (desmin staining) in WT (Q) and $PHD2^{+/-}$ (R) mice 24 hours after coronary artery occlusion**. S,** The quantification of the infarcted area (% of left ventricular area [LV]) shows reduced infarct size in $PHD2^{+/-}$ mice (R) compared to WT mice (Q) (N=4-5; P=0.03). **T,U,** Representative micrographs of infarcted areas (Sirius red) in WT (T) and $PHD2^{+/-}$ (U) hearts upon gelatin-bismuth-based angiographies (black spots). **V,W,** Collateral vessel area (V) and density (W) are increased in $PHD2^{+/-}$ hearts (U) compared to WT (T) in both remote healthy myocardium and infarct site (N=4-5; P=0.0002). Scale bars denote 50 µm in F-I; 100 µm in K,L; 1000 µm in Q,R; 50 µm in T,U. Asterisks in A,B,E,J,M,P,S,V, and W denote statistical significance versus WT. Error bars in A,B,E,J,M,P,S,V, and W show the standard error of the mean (SEM); all subsequent error bars are defined similarly.

FIGURE 2: ENHANCED COLLATERALIZATION IN PHD2$^{+/-}$ MUSCLES

A,B, Macroscopic view of gelatin-bismuth-based angiographies at baseline. PHD2$^{+/-}$ adductors (B) show comparable primary (blue arrow) and enhanced secondary (red arrow) and tertiary (black arrow) collateral vessels compared to WT (A) mice. The green arrow points to the femoral artery. **C,D,** PHD2$^{+/-}$ mice present increased number of secondary (C) and tertiary (D) collateral vessels, both at baseline and after ischemia (12 and 72 hours post-ischemia) (N=6-11; P<0.05). **E,F,** H&E staining of adductor sections after gelatin-bismuth-based angiography. Bismuth^{+} collaterals appear black. **G,H,** PHD2 haplodeficient mice present increased collateral vessel area (G) and density (H) compared to WT mice (N=8-14; P<0.01). **I,J,** Increased number of collaterals in PHD2$^{+/-}$ hindlimbs evaluated by X-ray radiography. **K-M,** Quantification of the micro-CT angiograms of hind limbs at baseline (K) showing increased number of large vessels (>200 μm in diameter) in the thigh of PHD2$^{+/-}$ (M) versus WT (L) mice (N=6; P=0.04). **N-P,** Quantification of micro-CT angiograms at baseline (N) showing increased number of large vessels (>200 μm in diameter) in PHD2$^{+/-}$ hearts (P) versus WT (O) hearts (N=6; P=0.04). **Q-T,** Morphometric analysis of α-smooth muscle actin (αSMA) collateral vessels in non-occluded and occluded adductor muscles of WT and PHD2$^{+/-}$ mice: **Q,** Density of αSMA^{+} collateral vessels (N=12; P<0.04); **R,** Total αSMA^{+} collateral area (N=12; P<0.05); **S,** Mean αSMA^{+} collateral vessel area (N=12; P<0.05). **T,** Thickness of the tunica media (N=8; P=0.04). **U-Y,** Staining of adductor sections for αSMA showing increased caliber and tunica media thickness of PHD2$^{+/-}$ collateral arteries at baseline; 72 hours after ligation, WT collaterals enlarge to the same size and thickness of PHD2$^{+/-}$ collaterals. Scale bars denote 50 μm in E,F and 10 μm in U,V,W,Y. Asterisks in C,D,G,H,K,N,Q,R,S, and T denote statistical significance versus WT. Hash signs in C,D,R,S, and T denote statistical significance compared to the baseline.

FIGURE 3: PHD2$^{+/-}$ MACROPHAGES DISPLAY A SPECIFIC PHENOTYPE

A,B, Quantification of leukocytes by CD45 immunostaining (A) and macrophages by F4/80 immunostaining (B) in adductor sections of WT and PHD2$^{+/-}$ mice at baseline and after

femoral artery ligation (N=8-20; P=NS). **C,** Histogram showing increased percentage of mannose receptor C, type 1^+ ($MRC1^+$) cells out of the $F4/80^+$ population in $PHD2^{+/-}$ adductors at baseline and 72 hours post-ligation (N=8; P=0.04 in baseline and N=8; P=0.03 in ischemia); $MRC1^+F4/80^+$ cells are significantly augmented in occluded WT and $PHD2^{+/-}$ limbs compared to the baseline (N=8; P<0.001 in WT mice; N=8; P=0.03 in $PHD2^{+/-}$ mice). **D-G,** Costaining of adductor sections for F4/80 (green), and MRC1 (red) quantified in C. Arrowheads in panels F and G point to F4/80 and MRC1 double positive cells. Collateral vessels are stained for αSMA (blue). **H,** Gene expression analysis (RT-PCR) in WT and $PHD2^{+/-}$ peritoneal macrophages (pMØ). PHD2 haplodeficiency upregulates some M2-like-markers, whereas some other M2-like-markers and all the M1-like genes tested are downmodulated (N=8-23, P<0.05). Data are expressed in fold change relative to WT, where the RNA levels in WT macrophages are represented by 1; all subsequent gene expression data are defined similarly, unless otherwise specified. **I,** Gene expression analysis (RT-PCR) in $F4/80^+$ tissue macrophages sorted from adductor muscles confirms increased levels of M2-markers (PDGFB, SDF1, Tie2, MMP2, Nrp1) in $PHD2^{+/-}$ mice at baseline (N=6; P<0.03). Seventy-two hours after femoral artery occlusion, RNA expression levels of all the genes tested, except SDF1 (N=6; P=0.01), caught up in WT macrophages (N=6; P=NS). Conversely, at baseline, PHD2 expression is about half in $PHD2^{+/-}$ versus WT macrophages; in ischemia (72 hours post-ligation), PHD2 expression in WT macrophages goes down to the levels in $PHD2^{+/-}$ macrophages, while it remains unchanged in $PHD2^{+/-}$ macrophages. Scale bars denote 20 μm in D,E,F and G. Asterisks in C,H and I denote statistical significance versus WT. Hash signs in A,B,C and I denote statistical significance compared to baseline.

FIGURE 4: MYELOID SPECIFIC DELETION OF ONE PHD2 ALLELE PREVENTS ISCHEMIC DAMAGE

A,B, Heterozygous deficiency of PHD2 in myeloid cells ($PHD2^{LysCre;lox/wt}$; labeled as lox/wt) increases the basal number of secondary (A) and tertiary (B) collateral branches (assessed by gelatin bismuth-based angiography) compared to both WT ($PHD2^{LysCre;wt/wt}$; labeled as wt/wt) and PHD2 homozygous deficiency ($PHD2^{LysCre;lox/lox}$; labeled as lox/lox) (N=18; P=0.01 and P=0.02, respectively). **C,D,** Histological quantification on adductor

sections of bismuth^{+} collateral vessel area (C) and density (D) at baseline (N=20; P=0.01 and P=0.003 respectively). **E,** Quantification of necrotic area (%) represented in F,G, and H (N=5-12; P=0.03). **F-H,** H&E staining of crural muscle sections showing that heterozygous (G), but not homozygous (H) deficiency of PHD2 in myeloid cells preserves perfusion (black spots of bismuth-gelatin) and thus protects fibers against ischemic necrosis when compared to wt/wt (F) mice. **I,** Heterozygous, but not homozygous loss of PHD2 in myeloid cells improves functional endurance (treadmill running test) 12 hours after ligation, despite comparable performance at baseline (N=5; P<0.05). **J,K,** Histograms showing collateral vessel density (J) and area (K) of non-occluded limbs 5 weeks after bone marrow transplantation. PHD2$^{+/-}$ bone marrow in WT and PHD2$^{+/-}$ recipient mice (HE→WT and HE→HE respectively) increases the number of bismuth^{+} collateral vessels at baseline; WT bone marrow transplants result in a lower number of collateral branches regardless of the genotype of the recipient mice (WT→WT and WT→HE). **L,** Quantification of ischemic necrosis 72 hours post-ischemia. **M,** The running capacity at 12 hours after femoral artery occlusion is increased in HE→WT mice compared to controls (WT→WT). Scale bars denote 100 μm in F,G, and H. Asterisks in A,B,C,D,E,I,J,K,L, and M denote statistical significance towards wt/wt and lox/lox (or WT→WT in J,K,L, and M).

FIGURE 5: PHD2$^{+/-}$ MACROPHAGE DERIVED SDF1 AND PDGFB PROMOTE ARTERIOGENESIS

A-D, Migration of primary endothelial cells (ECs) towards control medium (A), WT (B) and PHD2$^{+/-}$ (C) macrophages. Quantification of transmigrating ECs is represented in D (N=8; P=NS). **E-H,** Migration of primary smooth muscle cells (SMCs) towards control medium (E), WT (F) and PHD2$^{+/-}$ (G) macrophages. Quantification of transmigrating SMCs is represented in H (N=16; P<0.0001). **I,** Combined pharmacological inhibition of SDF1 pathway by AMD3100 and PDGFB pathway by imatinib reduces SMC migration towards PHD2$^{+/-}$ macrophages (N=8; P<0.02). **J,K,** SMC growth (J) is enhanced in presence of medium conditioned by PHD2$^{+/-}$ macrophages (N=4; P<0.001). Conversely, EC growth (K) is comparable (N=4; P=NS). **L-P,** The stimulation of SMCs with PHD2$^{+/-}$ macrophage-conditioned medium promotes a synthetic (proliferative) phenotype characterized by reduced RNA expression of calponin-1 (L), SM22α (M), smoothelin (N), NmMHC (O), and

αSMA (P) (N=4; P<0.001). **Q,** The pharmacological inhibition of SDF1 and PDGFB pathways, alone or in combination, prevents SMC growth induced by $PHD2^{+/-}$ macrophage-conditioned medium (N=4; P<0.05). **R,S,** Combined administration of AMD3100 and imatinib reduces more efficiently the formation of secondary (R) and tertiary (S) collateral vessels induced in HE→WT mice (N=8; P<0.05). Scale bars denote 50 μm in A,B,C,E,F, and G. Asterisks in H,I,J,L,M,N,O,P,Q,R, and S denote statistical significance versus WT (or WT→WT in R and S). Hash signs in D and H denote statistical significance towards control medium, in Q and S towards the baseline. Dollar sign in I,R, and S denotes statistical significance (P<0.01) towards the baseline and either treatment alone.

FIGURE 6: TEMS TRIGGER ARTERIOGENESIS IN $PHD2^{+/-}$ MICE VIA CANONICAL NF-κB PATHWAY

A, Quantification of $Tie2^{+}$ macrophages, infiltrating WT and $PHD2^{+/-}$ adductor muscle represented at baseline and 72 hours after ligation (N=8-14; P<0.04). **B,** The number of $Tie2^{+}$ circulating monocytes ($CD115^{+}Tie2^{+}$ double positive cells) is increased in $PHD2^{+/-}$ mice at baseline and 72 hours after ligation (N=6-14; P<0.01). **C,** Tie2 mRNA levels in WT and $PHD2^{+/-}$ circulating monocytes and tissue macrophages at baseline and 72 hours after femoral artery occlusion (N=4; P<0.05). **D,** Arterial growth (αSMA immunostaining) at baseline and after ischemia (day 3 and 7) in adductor sections of WT Tie2:tk-BMT and $PHD2^{+/-}$ Tie2:tk-BMT mice treated with saline or GCV. The administration of GCV completely abolishes the arterial vessel preconditioning observed in $PHD2^{+/-}$ Tie2:tk-BMT mice at baseline as well as after ischemia. In WT Tie2:tk-BMT mice, GCV prevents arterial growth occurring at 7 days post-ligation in the untreated group. **E,** At day 3 after femoral artery occlusion, GCV-treated $PHD2^{+/-}$ Tie2:tk-BMT mice present levels of fiber necrosis similar to those of WT Tie2:tk-BMT mice; GCV prevents healing of the tissue at 7 days post-ligation in both WT and $PHD2^{+/-}$ Tie2:tk-BMT mice (N=6; P<0.04). **F,** HIF-1α and HIF-2α accumulation in macrophages showing increased levels of HIF-1α and HIF-2α in PHD2 null ($PHD2^{LysCre;lox/lox}$), but not PHD2 haplodeficient ($PHD2^{LysCre;lox/wt}$) macrophages compared to control ($PHD2^{LysCre;wt/wt}$; N=4; P<0.001). Vinculin was used as loading control. **G,** NF-κB activity (luciferase reporter assay) is enhanced in $PHD2^{LysCre;lox/wt}$, but not in

$PHD2^{LysCre;lox/lox}$ macrophages. Silencing of PHD3 unleashes NFκB in $PHD2^{LysCre;lox/lox}$ macrophages. **H,** NF-κB is modulated by the hydroxylase activity of PHD2 in macrophages. The electroporation of $PHD2^{+/-}$ macrophages with a wild type PHD2 ($PHD2^{wt}$) blunts NF-κB activation, whereas a PHD2 construct containing a mutation at the catalytic site ($PHD2^{H313A}$) is not effective (N=4; P<0.05). **I,** $PHD2^{+/-}$ macrophages present enhanced NF-κB activity at baseline and upon TNF-α stimulation compared to WT macrophages (N=4; P<0.05). **J,** Western blot analysis of nuclear extracts from WT and $PHD2^{+/-}$ macrophages showing increased accumulation of both p65 (RelA) and p50 (NF-κB1) in $PHD2^{+/-}$ macrophages at baseline (N=3; P<0.05). **K,** Silencing of p65 or p50 inhibits NF-κB hyperactivation in $PHD2^{+/-}$ macrophages and combined knockdown of both subunits restores NF-κB function back to the WT levels (N=4; P<0.05). **L,** Genetic inactivation of IKKβ in PHD2 haplodeficient pMØ abrogates the upregulation of PDGFB, SDF1, and Tie2, while it did not have any effect on $PHD2^{wt/wt}$ macrophages (N=4; P<0.05). **M,** Histogram showing reduction of circulating $CD115^{+}Tie2^{+}$ double positive cells at baseline upon myeloid specific IKKβ gene targeting in myeloid specific PHD2 haplodeficient mice (N=6-12; P<0.05). **N,** αSMA immunostainings of adductor sections, revealing abrogation of collateral vessel preconditioning induced by PHD2 haplodeficiency upon myeloid specific IKKβ knockout; in WT mice, IKKβ gene deletion greatly prevented ischemia-induced arteriogenesis 7 days post-ligation (N=4-12, P<0.05). Asterisks in A,B,C,D,E,G,H,I,K,L,M, and N denote statistical significance (P<0.05). Hash signs in A,B,C,D,E,I, and N denote statistical significance compared to baseline, in G and K towards their scramble controls. Dollar signs in E denote statistical significance towards the baseline and GCV treatment, in K towards the baseline and either treatment alone.

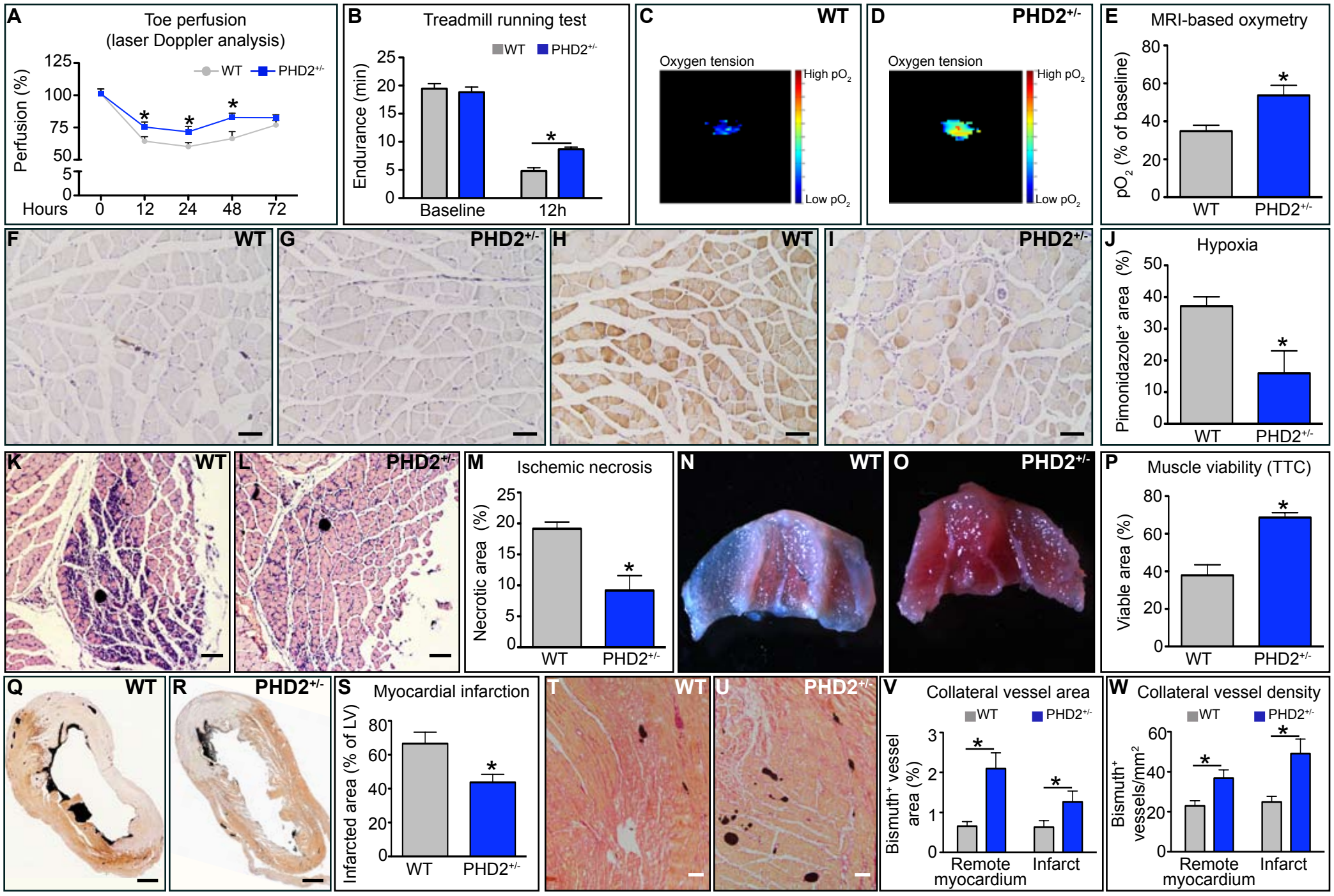
A
Toe perfusion
(laser Doppler analysis)
Perfusion (%)
125
100
75
50
5
0
Hours
0
12
24
48
72
WT
PHD2+/-
B
Treadmill running test
Endurance (min)
25
20
15
10
5
0
Baseline
12h
C
WT
Oxygen tension
High pO2
Low pO2
D
PHD2+/-
Oxygen tension
High pO2
Low pO2
E
MRI-based oxymetry
pO2 (% of baseline)
80
60
40
20
0
WT
PHD2+/-
F
WT
G
PHD2+/-
H
WT
I
PHD2+/-
J
Hypoxia
Pimonidazole+ area (%)
50
40
30
20
10
0
WT
PHD2+/-
K
WT
L
PHD2+/-
M
Ischemic necrosis
Necrotic area (%)
25
20
15
10
5
0
WT
PHD2+/-
N
WT
O
PHD2+/-
P
Muscle viability (TTC)
Viable area (%)
80
60
40
20
0
WT
PHD2+/-
Q
WT
R
PHD2+/-
S
Myocardial infarction
Infarcted area (% of LV)
80
60
40
20
0
WT
PHD2+/-
T
WT
U
PHD2+/-
V
Collateral vessel area
WT
PHD2+/-
Bismuth+ vessel area (%)
3
2
1
0
Remote myocardium
Infarct
W
Collateral vessel density
WT
PHD2+/-
Bismuth+ vessels/mm2
60
40
20
0
Remote myocardium
Infarct

Figure 1

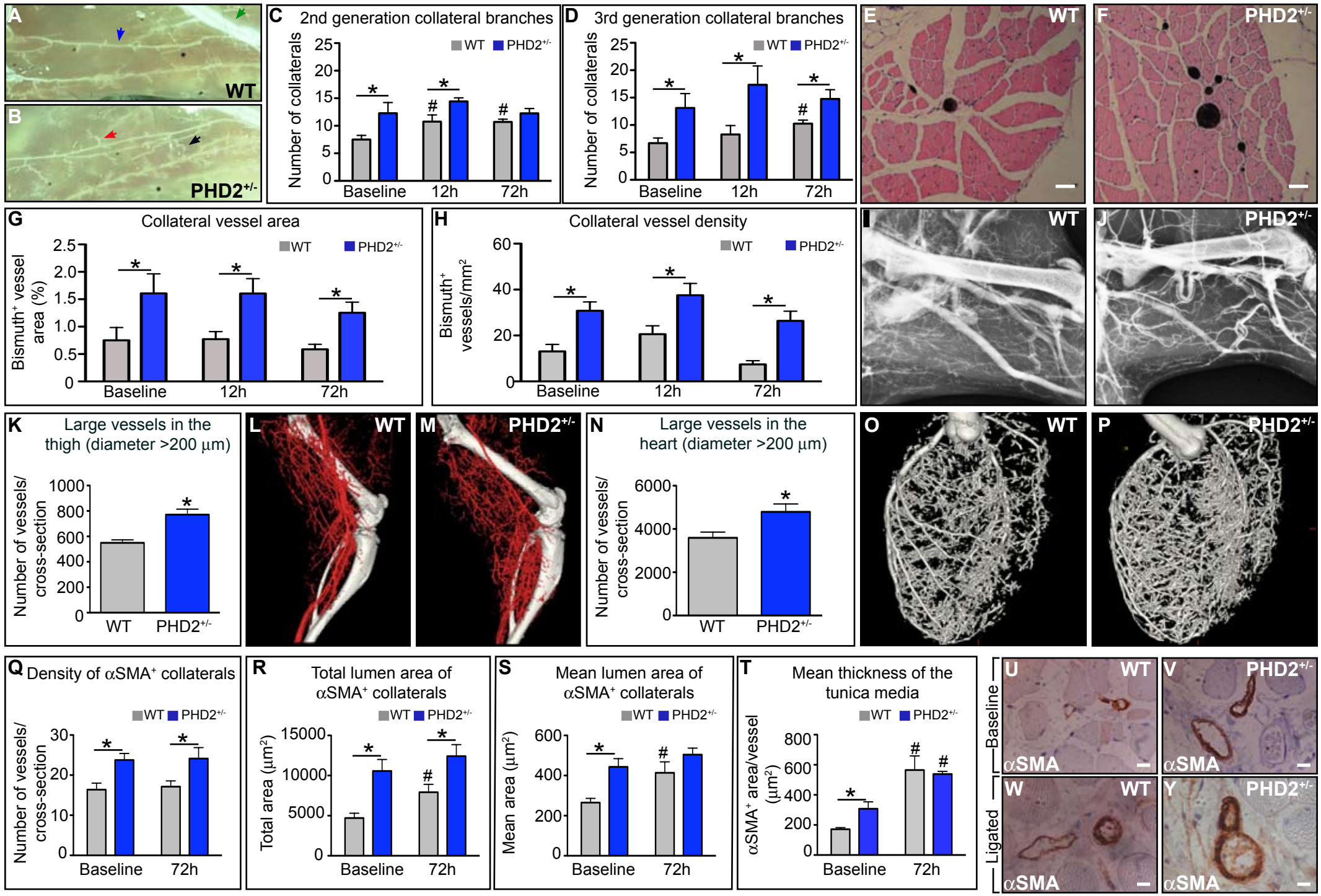
A
WT
B
PHD2+/-
C
2nd generation collateral branches
WT PHD2+/-
Number of collaterals
Baseline
12h
72h
D
3rd generation collateral branches
E
WT
F
PHD2+/-
G
Collateral vessel area
Bismuth+ vessel area (%)
H
Collateral vessel density
Bismuth+ vessels/mm2
I
J
K
Large vessels in the thigh (diameter >200 μm)
Number of vessels/ cross-section
L
M
N
Large vessels in the heart (diameter >200 μm)
O
P
Q
Density of αSMA+ collaterals
R
Total lumen area of αSMA+ collaterals
Total area (μm2)
S
Mean lumen area of αSMA+ collaterals
Mean area (μm2)
T
Mean thickness of the tunica media
αSMA+ area/vessel (μm2)
U
V
W
Y
Baseline
Ligated
αSMA

Figure 2

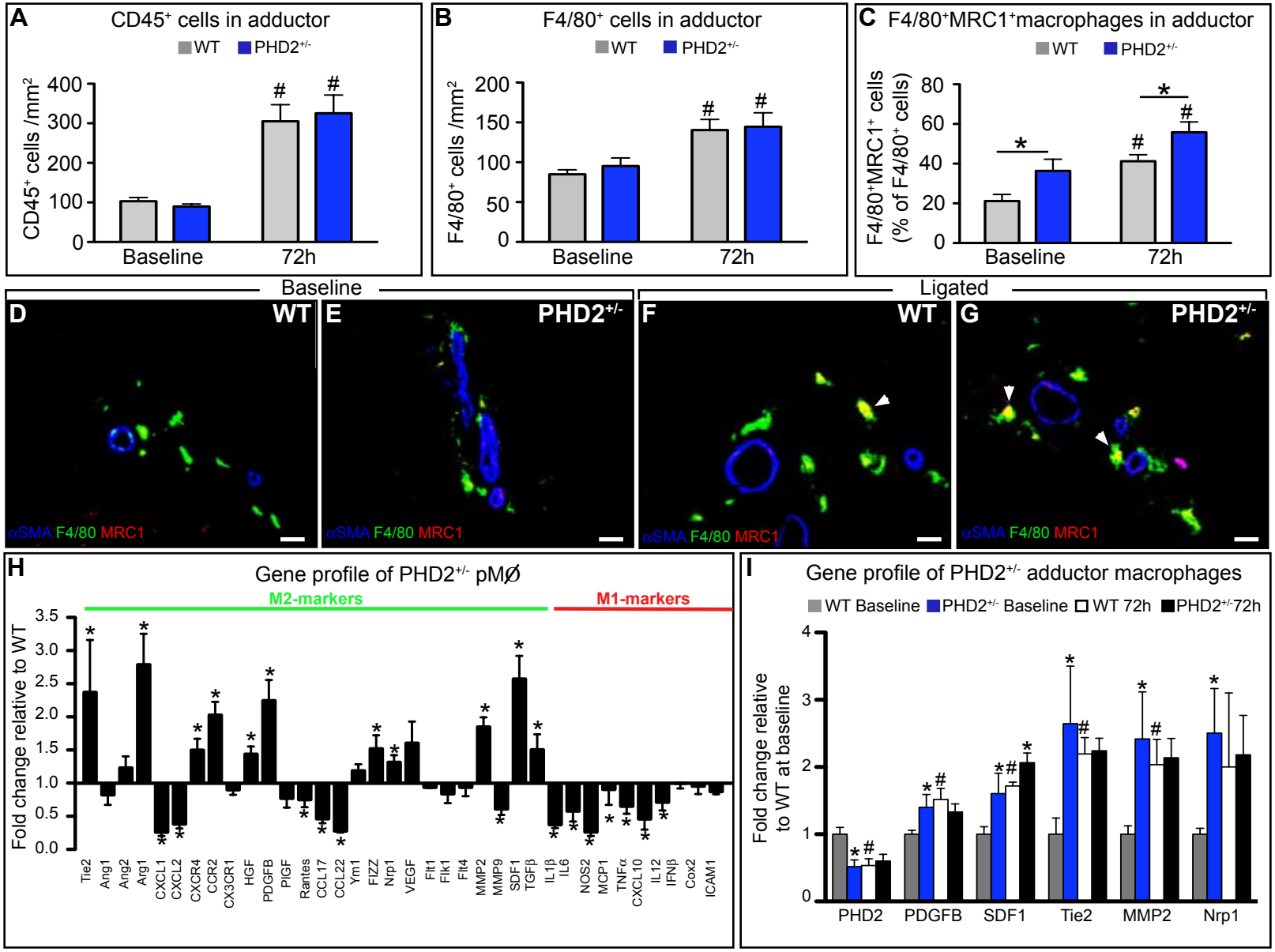
A
CD45+ cells in adductor
WT
PHD2+/-
CD45+ cells /mm2
400
300
200
100
0
#
#
Baseline
72h
B
F4/80+ cells in adductor
WT
PHD2+/-
F4/80+ cells /mm2
200
150
100
50
0
#
#
Baseline
72h
C
F4/80+MRC1+macrophages in adductor
WT
PHD2+/-
F4/80+MRC1+ cells (% of F4/80+ cells)
80
60
40
20
0
*
*
#
#
Baseline
72h
Baseline
Ligated
D
WT
αSMA F4/80 MRC1
E
PHD2+/-
αSMA F4/80 MRC1
F
WT
αSMA F4/80 MRC1
G
PHD2+/-
αSMA F4/80 MRC1
H
Gene profile of PHD2+/- pMØ
M2-markers
M1-markers
Fold change relative to WT
3.5
3.0
2.5
2.0
1.5
1.0
0.5
0.0
Tie2
Ang1
Ang2
Arg1
CXCL1
CXCL2
CXCR4
CCR2
CX3CR1
HGF
PDGFB
PlGF
Rantes
CCL17
CCL22
Ym1
FIZZ
Nrp1
VEGF
Flt1
Flk1
Flt4
MMP2
MMP9
SDF1
TGFβ
IL1β
IL6
NOS2
MCP1
TNFα
CXCL10
IL12
IFNβ
Cox2
ICAM1
I
Gene profile of PHD2+/- adductor macrophages
WT Baseline
PHD2+/- Baseline
WT 72h
PHD2+/-72h
Fold change relative to WT at baseline
4
3
2
1
0
PHD2
PDGFB
SDF1
Tie2
MMP2
Nrp1

Figure 3

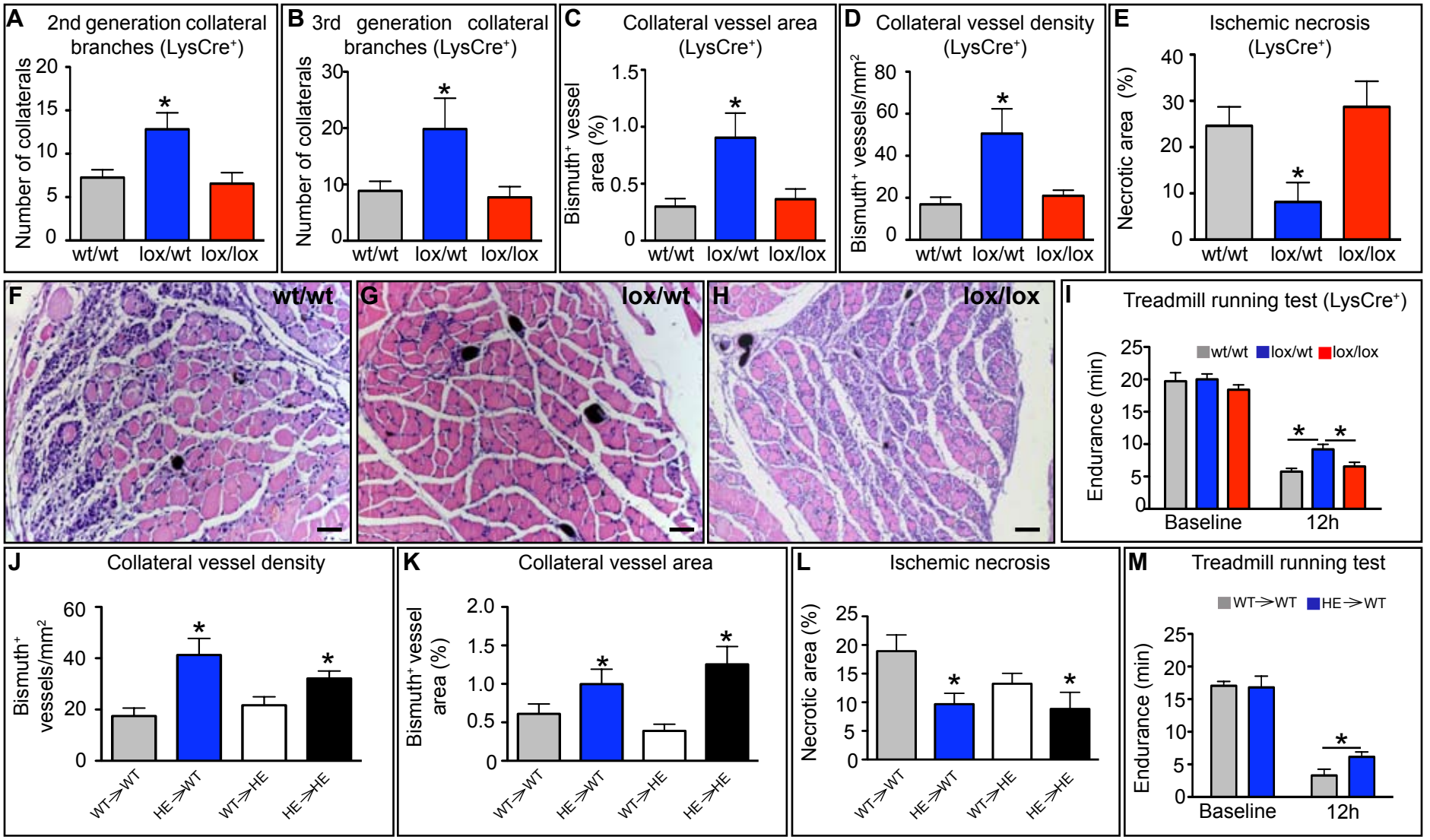
A
2nd generation collateral branches (LysCre+)
Number of collaterals
wt/wt
lox/wt
lox/lox
B
3rd generation collateral branches (LysCre+)
Number of collaterals
C
Collateral vessel area (LysCre+)
Bismuth+ vessel area (%)
D
Collateral vessel density (LysCre+)
Bismuth+ vessels/mm2
E
Ischemic necrosis (LysCre+)
Necrotic area (%)
F
wt/wt
G
lox/wt
H
lox/lox
I
Treadmill running test (LysCre+)
Endurance (min)
Baseline
12h
J
Collateral vessel density
Bismuth+ vessels/mm2
WT→WT
HE→WT
WT→HE
HE→HE
K
Collateral vessel area
Bismuth+ vessel area (%)
L
Ischemic necrosis
Necrotic area (%)
M
Treadmill running test
WT→WT
HE→WT
Endurance (min)
Baseline
12h

Figure 4

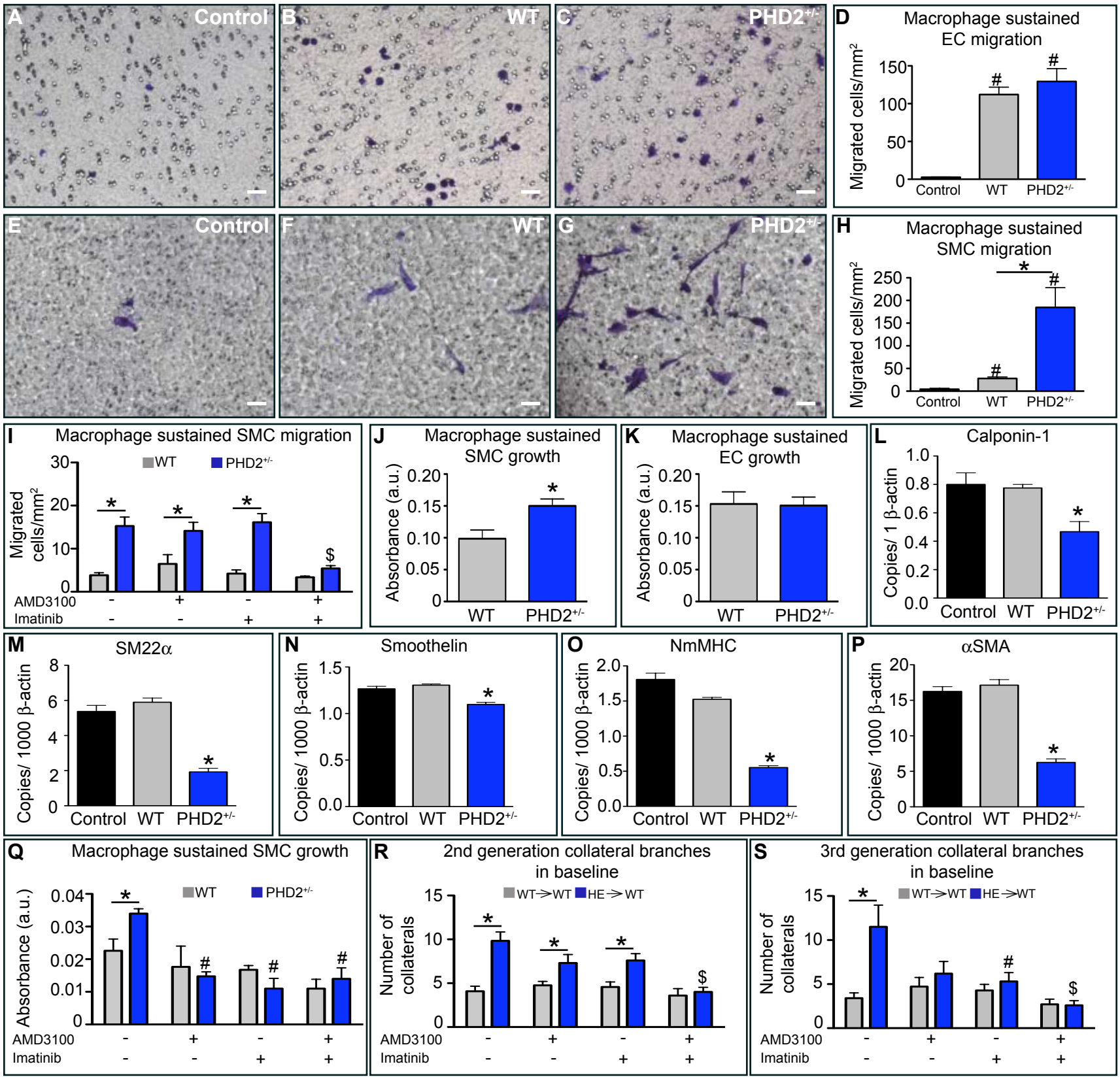
A Control
B WT
C PHD2+/-
D Macrophage sustained EC migration
Migrated cells/mm2
Control WT PHD2+/-
E Control
F WT
G PHD2+/-
H Macrophage sustained SMC migration
Migrated cells/mm2
Control WT PHD2+/-
I Macrophage sustained SMC migration
WT PHD2+/-
Migrated cells/mm2
AMD3100
Imatinib
J Macrophage sustained SMC growth
Absorbance (a.u.)
WT PHD2+/-
K Macrophage sustained EC growth
Absorbance (a.u.)
WT PHD2+/-
L Calponin-1
Copies/ 1 β-actin
Control WT PHD2+/-
M SM22α
Copies/ 1000 β-actin
Control WT PHD2+/-
N Smoothelin
Copies/ 1000 β-actin
Control WT PHD2+/-
O NmMHC
Copies/ 1000 β-actin
Control WT PHD2+/-
P αSMA
Copies/ 1000 β-actin
Control WT PHD2+/-
Q Macrophage sustained SMC growth
Absorbance (a.u.)
WT PHD2+/-
AMD3100
Imatinib
R 2nd generation collateral branches in baseline
WT→WT HE→WT
Number of collaterals
AMD3100
Imatinib
S 3rd generation collateral branches in baseline
WT→WT HE→WT
Number of collaterals
AMD3100
Imatinib

Figure 5

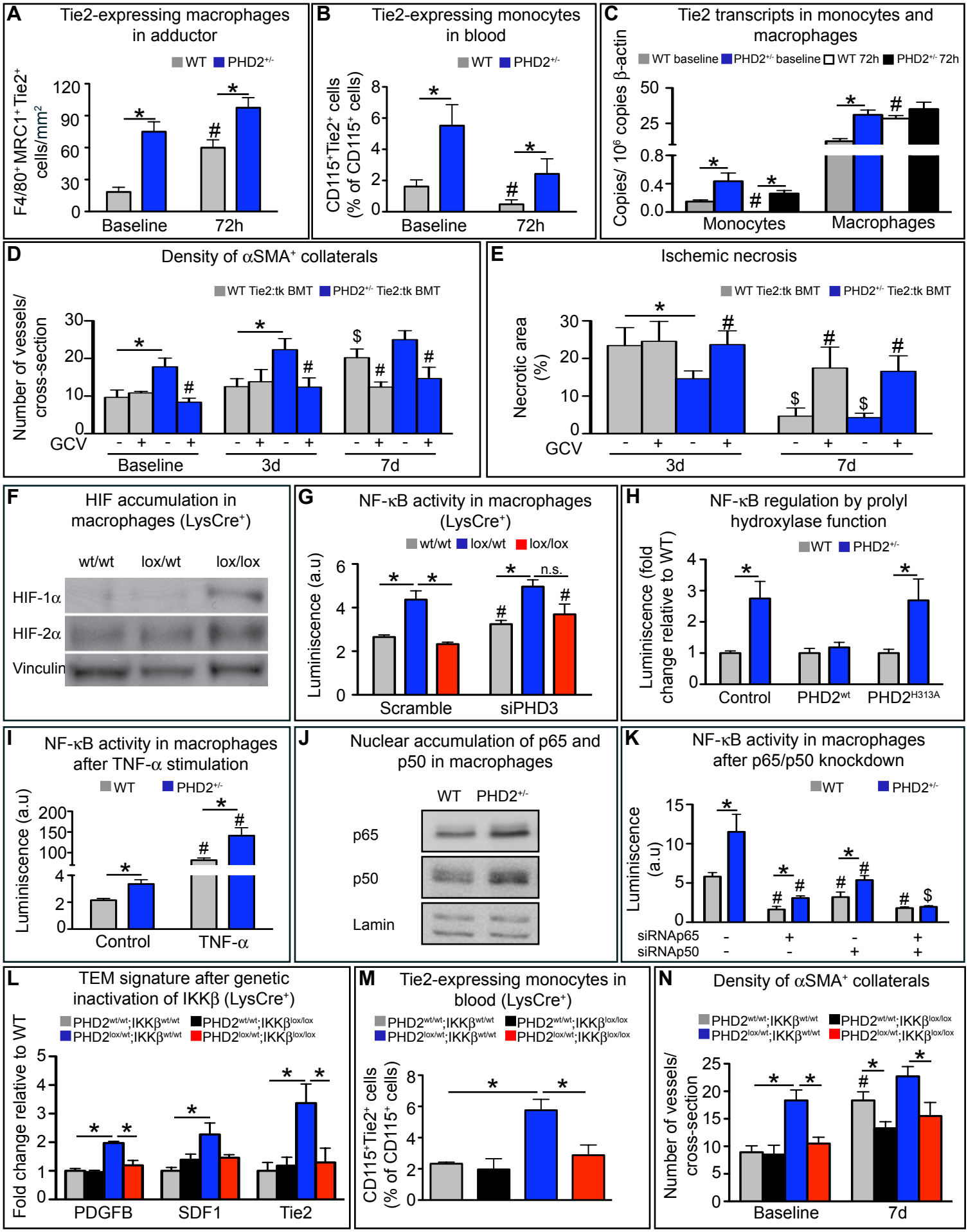
A
Tie2-expressing macrophages in adductor
WT PHD2+/-
F4/80+ MRC1+ Tie2+ cells/mm2
120
90
60
30
0
Baseline
72h
B
Tie2-expressing monocytes in blood
WT PHD2+/-
CD115+Tie2+ cells (% of CD115+ cells)
8
6
4
2
0
Baseline
72h
C
Tie2 transcripts in monocytes and macrophages
WT baseline PHD2+/- baseline WT 72h PHD2+/- 72h
Copies/ 10^6 copies β-actin
50
25
0.8
0.4
0.0
Monocytes
Macrophages
D
Density of αSMA+ collaterals
WT Tie2:tk BMT PHD2+/- Tie2:tk BMT
Number of vessels/ cross-section
30
20
10
0
GCV
Baseline
3d
7d
E
Ischemic necrosis
WT Tie2:tk BMT PHD2+/- Tie2:tk BMT
Necrotic area (%)
30
20
10
0
GCV
3d
7d
F
HIF accumulation in macrophages (LysCre+)
wt/wt
lox/wt
lox/lox
HIF-1α
HIF-2α
Vinculin
G
NF-κB activity in macrophages (LysCre+)
wt/wt lox/wt lox/lox
Luminiscence (a.u)
6
4
2
0
n.s.
Scramble
siPHD3
H
NF-κB regulation by prolyl hydroxylase function
WT PHD2+/-
Luminiscence (fold change relative to WT)
4
3
2
1
0
Control
PHD2wt
PHD2H313A
I
NF-κB activity in macrophages after TNF-α stimulation
WT PHD2+/-
Luminiscence (a.u)
200
150
100
4
2
0
Control
TNF-α
J
Nuclear accumulation of p65 and p50 in macrophages
WT PHD2+/-
p65
p50
Lamin
K
NF-κB activity in macrophages after p65/p50 knockdown
WT PHD2+/-
Luminiscence (a.u)
15
10
5
0
siRNAp65
siRNAp50
L
TEM signature after genetic inactivation of IKKβ (LysCre+)
PHD2wt/wt;IKKβwt/wt PHD2wt/wt;IKKβlox/lox
PHD2lox/wt;IKKβwt/wt PHD2lox/wt;IKKβlox/lox
Fold change relative to WT
5
4
3
2
1
0
PDGFB
SDF1
Tie2
M
Tie2-expressing monocytes in blood (LysCre+)
PHD2wt/wt;IKKβwt/wt PHD2wt/wt;IKKβlox/lox
PHD2lox/wt;IKKβwt/wt PHD2lox/wt;IKKβlox/lox
CD115+Tie2+ cells (% of CD115+ cells)
8
6
4
2
0
N
Density of αSMA+ collaterals
PHD2wt/wt;IKKβwt/wt PHD2wt/wt;IKKβlox/lox
PHD2lox/wt;IKKβwt/wt PHD2lox/wt;IKKβlox/lox
Number of vessels/ cross-section
25
20
15
10
5
0
Baseline
7d

Figure 6

SUPPLEMENTARY INFORMATION

MACROPHAGE SKEWING BY PHD2 HAPLODEFICIENCY PREVENTS ISCHEMIA BY INDUCING ARTERIOGENESIS

Yukiji Takeda, Sandra Costa, Estelle Delamarre, Carmen Roncal, Rodrigo Leite De Oliveira, Mario Leonardo Squadrito, Veronica Finisguerra, Françoise Bruyère, Sofie Deschoemaeker, Mathias Wenes, Alexander Hamm, Jens Serneels, Julie Magat, Tapan Bhattacharrya, Andrey Anisimov, Benedicte F. Jordan, Kari Alitalo, Patrick Maxwell, Bernard Gallez, Zhenwu Zhuang, Yoshihiko Saito, Michael Simons, Michele De Palma & Massimiliano Mazzone

SUPPLEMENTARY METHODS

ANIMALS: 129/S6 or Balb/C WT and PHD2$^{+/-}$ mice (8-12 weeks old) were obtained from our mouse facility. PHD2$^{+/-}$ and PHD2 conditional knock-out mice were obtained as previously described[1]. VE-Cadherin:CreERT and PDGFRB:Cre transgenic mice were generated by Dr. Adams at the Cancer Research UK (London, UK), currently at the Max-Planck-Institute (Munster, Germany)[2,3]. IKKβ conditional knock-out mice were obtained from Dr. Karin (UCSD, California)[4]. Tie2:Cre and Rosa26:CreERT transgenic mice were purchased by the Jackson Laboratory. Housing and all experimental animal procedures were approved by the Institutional Animal Care and Research Advisory Committee of the K.U.Leuven.

MOUSE MODEL OF HINDLIMB ISCHEMIA: To induce hindlimb ischemia, unilateral or bilateral ligations of the femoral artery and vein (proximal to the popliteal artery) and the cutaneous vessels branching from the caudal femoral artery side branch were performed without damaging the nervus femoralis[5]. By using this procedure, collateral flow to adductor muscles is preserved via arterioles branching from the femoral artery, therefore 50% up to 60% of perfusion is preserved by this method. Two superficial preexisting collateral arterioles, connecting the femoral and saphenous artery, were used for analysis. Functional perfusion measurements of the collateral region were performed using a Lisca PIM II camera (Gambro). Gelatin-bismuth-based angiography was performed as described[6] and analyzed by photoangiographs (Nikon D1 digital camera). Collateral side branches were categorized as follows: second-generation collateral arterioles directly branched from the main collateral, whereas third-generation collateral arterioles were orientated perpendicularly to the second-generation branches. The number of secondary and tertiary collateral arterioles was counted. After perfusion-fixation, the muscle tissue between the 2 superficial collateral arterioles (adductor) was post-fixed in 2% paraformaldehyde (PFA), paraffin-embedded, and morphometrically analyzed. An endurance treadmill-running test was performed at baseline and 12 hours post-bilateral-ligation.

MOUSE MODEL OF MYOCARDIAL INFARCTION: Myocardial infarction (MI) was induced by permanent ligation of the left anterior descending coronary artery as previously

described[7]. Briefly, animals were anesthetized with pentobarbital (100 mg/kg i.p.), fixed in the supine position and the trachea was intubated with a 1.1-mm steel tube. Positive pressure respiration (1.5-2 ml, 70 strokes/min) was started and the left thorax was opened in the fourth intercostal space. All muscles overlying the intercostal space were dissected and retracted with 5-0 silk threads; only the intercostal muscles were transected. After opening the pericardium, the main left coronary artery, which was clearly visible, was ligated just proximal to the main bifurcation by using 6-0 silk and an atraumatic needle (Ethicon K801). Infarction was evident from discoloration of the ventricle. The thorax was closed and the skin sutured with 5-0 silk. Animals recovered at 30ºC. Gelatin-bismuth-based angiography was performed 24 hours after ligation and hearts were then collected in 2% PFA.

OXYMETRY: Oxygen tension (pO_2) in the lower limb was measured using ^{19}F-MRI oxymetry in non-ligated and ligated legs 12 hours after femoral artery ligation. The oxygen reporter probe hexafluorobenzene (HFB) was injected directly into the crural muscle. MRI was performed with a 4.7T (200 MHz, ^{1}H), 40 cm inner diameter bore system (Bruker Biospec). A tunable $^{1}H/^{19}F$ surface coil was used for radiofrequency transmission and reception[8].

HISTOLOGY, IMMUNOSTAINING, AND MORPHOMETRY: Adductor, crural muscles and hearts were dissected, fixed in 2% PFA, dehydrated, embedded in paraffin, and sectioned at 7-μm-thickness. Area of necrotic tissues in the crural muscle was analyzed by Hematoxylin & Eosin (H&E) staining. Necrotic cells display a more glassy homogeneous appearance in the cytoplasm with increased eosinophilia, while the nuclear changes are reflected by karyolysis, pyknosis, and karyorrhexis. Necrotic area was defined as the percentage of area which includes these necrotic myocytes, inflammatory cells, and interstitial cells, compared to the total soleus area. Infarct size was measured in desmin stained hearts 24 hours after ischemia as previously described[9]. After deparaffinization and rehydration, sections were blocked and incubated overnight with primary antibodies: rat anti-CD31, dilution 1/500 (BD-pharmingen), mouse anti-aSMA, dilution 1/500 (Dako), rat anti-F4/80, dilution 1/100 (Serotec), dilution 1/50 (BD-pharmingen), rat anti-CD45, dilution 1/100 (BD-pharmingen), goat anti-MRC1, dilution 1/200 (R&D), rat anti-Tie-2, dilution 1/100 (Reliatech), rabbit anti-desmin dilution 1/150 (Cappel). In order

to analyze capillary density and area, images of CD31 stained sections of the entire soleus were taken at 40x. In order to measure bismuth-positive vessel density and area, H&E stained paraffin sections were analyzed and vessels filled with bismuth-gelatin (black spots) were taken in account. Images of the entire soleus were acquired at 20x for this analysis. The values in the graph represent the averages of the mean vessel density and area per soleus muscle. The same method was used to quantify vessel capillaries and collateral branches in cardiac tissues. Density and area were measure by using a KS300 (Leica) software analysis. Hypoxic cells were analyzed 2 hours after injection of 60 mg/kg pimonidazole into operated mice. Mice were sacrificed and muscles were harvested. Paraffin sections were stained with Hypoxiprobe-1-Mab-1 (Hypoxiprobe kit; Chemicon International) following the manufacturer's instructions. Oxidative stress and proliferation rate were assessed on 7μm-thick cryosections by using the goat anti-8-OHdG antibody, dilution 1/200 (Serotec) and the rat anti-BrdU antibody, dilution 1/300 (Serotec). Sections were subsequently incubated with appropriate secondary antibodies, developed with fluorescent dies or 3,3'-disminobenzidine (DAB, Sigma). Whole muscle viability was assessed on unfixed 2-mm-thick tissue slices by staining with 2,3,5-triphenyltetrazolium chloride (TCC). Viable area, stained in red, was traced and analyzed. Pictures for morphometric analysis were taken using a Retiga EXi camera (Q Imaging) connected to a Nikon E800 microscope or a Zeiss Axio Imager connected to an Axiocam MRc5 camera (Zeiss) and analysis was performed using KS300 (Leica). Angiograms were obtained by X-Ray and CT angiographies of hearts and legs at baseline.

MACROPHAGE PREPARATION: To harvest peritoneal macrophages (pMØ), the peritoneal cavity was washed with 5 ml of RPMI 10% FBS. The pooled cells were then seeded in RPMI 10% FBS in 6-well plates ($2x10^6$ cells/well), 12-well plates ($1x10^6$ cells/well), or 24-well plates ($5x10^5$ cells/well). After 6 hours of incubation at 37°C in a moist atmosphere of 5% CO_2 and 95% air, non-adhering cells on each plate were removed by rinsing with phosphate-buffered saline (PBS). The attached macrophages were cultured in different media for 12 hours or 48 hours depending on the experiments performed, as described below. When high amounts of cells were needed (analysis for HIF accumulation and NF-κB activity), macrophages were derived from bone marrow

precursors as described before[10]. Briefly, bone marrow cells ($2x10^6$ cells/ml) were cultured in a volume of 5 ml in a 10 cm Petri dish (non tissue culture treated, bacterial grade) for 7 to 10 days in DMEM supplemented with 20% FBS and 30% L929 conditioned medium as a source of M-CSF. The cells obtained in those cultures are uniformly macrophages. Tamoxifen-inducible PHD2 haplodeficient pMØ ($PHD2^{Rosa26CreERT;lox/wt}$) were isolated as described above. After 8 hours in culture (RPMI, 10% FBS), pMØ were washed twice with PBS and treated with or without 2 μM 4-hydroxytamoxifen (4-OHT, Sigma) in complete medium for 48 hours to allow Cre recombinase activity. Cells were then washed and kept in culture for other 48 hours before mRNA isolation and gene expression analysis.

QUANTITATIVE PCR ANALYSIS: In order to investigate gene expression in pMØ, quantitative RT-PCR was performed. After preparing pMØ, the cells were cultured in normoxic condition for 12 hours and RNA was extracted. To analyze the expression levels of chemoattractants in the adductor, tissues were collected at baseline or 24 hours post-ischemia and RNA was extracted. Macrophages and ECs were freshly sorted from dissected adductors as described below and RNA was extracted. Quantitative RT-PCR was performed with commercially available or home-made primers and probes for the studied genes. The assay ID (Applied Biosystems, Foster City, CA) or the sequence of primers and probes (when home-made) are listed in Supplementary Table 5. RNA levels of Tie-2, SDF1, and PDGFB after inhibition of NF-kB pathway were measured by RT-PCR on pMØ exposed for 12 hours to 500 nM 6-amino-4-(4-phenoxyphenylethylamino)quinazoline.

PROTEIN EXTRACTION AND IMMUNOBLOT: Protein extraction was performed using 8M urea buffer (10% glycerol, 1% SDS, 5 mM DTT, 10mM Tris-HCl, pH 6.8) as previously described[1]. Nuclear proteins were extracted in 1% SDS buffer upon cytoplasmic separation by using a hypotonic lysis buffer (10 mM KCl, 10 mM EDTA, 0.5% NP40, 10 mM HEPES, pH=8, supplemented with phosphatase and protease inhibitors, from Roche). Signal was detected using ECL system (Invitrogen) according to the manufacture's instructions. The following antibodies were used: rabbit anti-HIF-1α (Novus), rabbit anti-p105/50, rabbit anti-HIF-2α (Abcam), PM9 rabbit anti-HIF-2α (from

Dr. Maxwell), mouse anti-vinculin (Sigma), rabbit anti-lamin A/C, rabbit anti-p65 (Cell Signaling).

TRANSDUCTION AND TRANSFECTION OF BONE MARROW DERIVED MACROPHAGES AND LUNG ENDOTHELIAL CELLS: To express an inducible NF-κB responsive firefly luciferase reporter, commercially available lentiviral vector particles (LV) were used (Cignal Lenti NF-κB Reporter; SABiosciences). $2.5x10^5$ bone marrow derived macrophages and 10^5 primary lung endothelial cells (isolated as previously described[1]) were seeded in a 24-well plate in DMEM 10% FBS or M199 20% FBS for 8 hours. Cells were transduced with 10^8 TU/ml. Eight hours after transduction, the medium was replaced. After 48 hours, cells were stimulated with TNFα (20 ng/mL) for 8 hours and the same amount of protein extract was read in a luminometer. For PHD3 silencing, siRNA oligonucleotides were designed using the Invitrogen online siRNA design tool (http://rnaidesigner.invitrogen.com). The following sequences (sense strands) and target positions were used: PHD3 siRNA: 5'-GCCGGCUGGGCAAAUACUAUGUCA-3'; scramble siRNA:5'-CACCGCTTAACCCGTATTGCCTAT-3'. In brief, one day after the transduction of macrophages with LV, cells were transfected using Lipofectamine 2000 (Invitrogen) according to the manufacturer's instructions. Preparation of the oligonucleotide-Lipofectamine 2000 complexes was done as followed: 25 pmol siRNA oligonucleotide (stock: 20 µM) was diluted in 50 µl Opti-MEM I reduced serum medium. Lipofectamine 2000 (1.5 µl) was diluted in 50 µl Opti-MEM I reduced serum medium and incubated for 5 minutes at room temperature. siRNA oligonucleotides were gently mixed with Lipofectamine 2000 and allowed to incubate at room temperature for 20 minutes to form complexes. Just before transfection, the cell culture medium was removed and cells were rinsed twice with serum-free Opti-MEM I medium. The Lipofectamine 2000-siRNA oligonucleotide complexes were added to each well in 400 µl of serum-free Opti-MEM medium for 5 hours. Afterwards, cells were incubated in complete medium for 48 hours at 37°C in a CO_2 incubator and assayed for gene knockdown (RT-PCR) and luciferase activity. To assess if the increased NF-κB activity observed in $PHD2^{+/-}$ macrophages was dependent on the hydroxylase activity of PHD2, 48h before

transduction, $4x10^6$ bone marrow derived macrophages were resuspended in 240 μl of Opti-MEM and were electroporated (250V, 950uF,∞ Ω) with 7 μg of plasmids expressing a wild type PHD2 ($PHD2^{wt}$) or a PHD2 containing a mutation at the catalytic site ($PHD2^{H313A}$). Silencing of the canonical pathway subunits p65 (RelA) and p50 (NF-κB1) was achieved by electroporation with specific siRNAs. Briefly, 48h before transduction, $2.4x10^6$ bone marrow derived macrophages were resuspended in 320 μl of Opti-MEM and were electroporated (250V, 950μF, ∞Ω) with 60 pmol of siRNA for either scramble, p65, p50, or combination of p50 and p65. For higher efficiency of silencing, two different siRNA sequences for each respective gene were designed (http://rnaidesigner.invitrogen.com). For p65: 5'-TGTCTGCACCTGTTCCAAATT-3' and 5'-TGCTGATGGAGTACCCTGATT-3'; for p50: 5'-GAATACTTCATGTGACTAATT-3' and 5'-CAAAGGTTATCGTTCAGTTTT-3'; for the scramble siRNA: 5'-CACCGCTTAACCCGTATTGCCTAT-3'.

CELL MIGRATION AND VIABILITY ASSAYS: Migration and proliferation of SMCs and ECs were assessed by using 8μm-pore Transwell permeable plate for migration assays and 0.4μm-pore Transwell permeable plate for proliferation assays (Corning Life Science). To determine cell migration towards the factors secreted by pMØ, pMØ were cultured in the lower chamber for 12 hours in RPMI 1% FBS or in M-199 1% FBS (migration assay), or 48 hours in DMEM-F12 1% FBS or in M-199 1% FBS (proliferation assay). For migration assays, hCASMC (Human coronary artery smooth muscle cells; from Lonza) and HUVEC (Human umbilical vein endothelial cells; from Lonza) were starved for 12 hours in their own medium at 1% FBS and then seeded in the upper chamber ($5x10^3$ cells in 200 μl of medium 1% FBS), with or without AMD3100 (1 μg/ml, Sigma-Aldrich, Dorset, U.K) and/or imatinib (2.5 μg/ml, Novartis). SMCs and HUVECs were incubated for 2 days or 24 hours respectively, and migrated cells were fixed with 4% PFA, stained with 0.25% crystal violet/ 50% methanol and counted under the microscope. VEGF (100 ng/mL, R&D), PDGFB (100 ng/mL, R&D), or SDF1 (100 ng/mL, R&D) were used as positive controls. For cell growth assays, RAOSMC (Rat Aortic Smooth Muscle Cells) and HUVEC were seeded on the upper chambers ($5x10^3$ cells/ transwell) and cultivated with pMØ for 24 hours in DMEM-F12 1% FBS or M-199 1%

FBS for RAOSMC and HUVEC cells, respectively. The cell proliferative ability was then analyzed using WST-1 Cell Proliferation Assay (Roche Applied Biosciences) according to the manufacturer instructions. Alternatively, WT and $PHD2^{+/-}$ pMØ were seeded in the lower chamber of a Transwell and transduced with lentiviral vectors (10^8 TU/ml; Sigma) carrying an shRNA against SDF1, PDGFB, or a scramble control (purchased from Sigma). Sixty hours after macrophage transduction, SMC migration or growth assays were performed by seeding the SMCs in the upper side of the Transwell as described above.

SMC DIFFERENTIATION ASSAY: pMØ were seeded in a 24-well plate with DMEM F-12 5% FBS. Conditioned medium was harvested after 2 days and supplemented with 25 mM HEPES. RAOSMC were seeded in a 24-well plate ($80x10^3$ cells/ well) and incubated for 5 hours at 37°C in a moist atmosphere of 5% CO_2 and 95% air. After 2 hours of starvation in DMEM-F12 1% FBS, SMC were stimulated with conditioned medium from WT and $PHD2^{+/-}$ pMØ. After 24 hours, differentiation status of the SMCs was assessed by RT-PCR.

FACS ANALYSIS AND MACROPHAGE AND ENDOTHELIAL CELL SORTING: FACS analysis of circulating TEMs was performed in 200 μl of peripheral blood, harvested by eye bleeding at baseline or 3 days after femoral artery ligation. Blood samples were incubated for 20 minutes at 4°C with a rat APC-conjugated anti-CD115, a mouse PE-conjugated anti-Tie2 (eBiosciences), or a rat FITC conjugated anti-Gr1 (BD-pharmingen). For cell sorting of adductor macrophages and ECs, the adductors were dissected, dissociated mechanically, and digested using collagenase I for 45 minutes at 37°C. For macrophage sorting, the digested cell suspension was incubated for 15 minutes with mouse anti-CD16/CD32 mAb (Fc Block™, BD-pharmingen) and stained with rat FITC-conjugated anti-F4/80 antibody (Serotec) for 20 minutes at 4 °C. $CD31^+CD45^-$ endothelial cells were sorted from the digested adductor cell suspension after incubation with rat APC-conjugated anti-CD31 and rat FITC-conjugated anti-CD45 (BD-pharmingen) for 20 minutes at 4 °C.

BONE MARROW (BM) TRANSPLANTATION AND HEMATOLOGICAL ANALYSIS: Balb/c WT and $PHD2^{+/-}$ recipient mice were irradiated with 7.5 Gy. Subsequently, 5×10^6 bone marrow

cells from green fluorescent protein^{+} (GFP^{+}) WT or GFP^{+} PHD2$^{+/-}$ mice were injected intravenously via the tail vein. After one week, saline or AMD3100 (5mg/kg) was administered intravenously and saline or imatinib (50mg/ml) was administered by oral gavage for 4 weeks. Femoral artery ligation, treadmill running test, and bismuth angiography were performed at 6 weeks after bone marrow reconstitution. Red and white blood cell count was determined using a hemocytometer (Cell-Dyn 3700, Abbott) on peripheral blood collected in heparin by retro-orbital bleeding. To assess the effect of acute deletion of macrophage borne PHD2 on arteriogenesis, PHD2$^{Rosa26CreERT;lox/wt}$ bone marrows were transplanted into lethally irradiated WT recipient mice. After five weeks, transplanted mice were injected i.p. with tamoxifen (1 mg/mouse; Sigma) or vehicle for 5 days. TEM quantification and femoral artery ligation were performed 10 days after tamoxifen treatment as explained above.

BONE MARROW-DERIVED, LINEAGE NEGATIVE HEMATOPOIETIC CELL ISOLATION, TRANSDUCTION AND TRANSPLANTATION: Six to 12-week–old WT or PHD2$^{+/-}$ Balb/C mice were killed and their BM was harvested by flushing the femurs and the tibias. Lineage-negative cells (lin^{-} cells) enriched in hematopoietic stem/progenitor cells (HS/PCs) were isolated from BM cells using a cell purification kit (StemCell Technologies) and transduced by concentrated lentiviral vectors. Briefly, 10^6 cells/ml were pre-stimulated for 4-6 hours in serum-free StemSpan medium (StemCell Technologies) containing a cocktail of IL-3 (20 ng/ml), SCF (100 ng/ml), TPO (100 ng/ml), and FLT-3L (100 ng/ml) (all from Peprotech), and transduced with 10^8 TU/ml of two lentiviral vectors (LVs), Tie2:tk (to deplete TEMs in transplanted mice) and PGK:GFP (to assess the efficiency of BM reconstitution in transplanted mice). After 12 hours, 10^6 cells were washed and infused into the tail vein of lethally irradiated 6-week-old female Balb/C mice (radiation dose: 7.5 Gy).

VECTOR COPY NUMBER ANALYSIS: Transduced lin^{-} cells were cultured and collected after 9 days while blood from the transplanted mice was collected 4 weeks after HS/PCs tail vein injection to measure the number of integrated LV copies/cell genome (vector copy number, VCN) by RT-PCR as previously described[11]. Briefly, for vector copy number (VCN) analysis, we performed RT-PCR using custom TaqMan assays specific for β-actin, HSV-tk, or HIV-gag sequences (Applied Biosystems). Standard curves for HSV-tk

(contained by Tie2:tk LV) or HIV-gag (contained by both Tie2:tk and PGK:GFP LVs) were obtained from genomic DNA samples containing known amounts of integrated LV. The VCN of genomic DNA standard curves was determined using custom TaqMan assays specific for LVs (Applied Biosystems). The SDS 2.2.1 software was used to extract raw data (CT) and to perform VCN analysis. To calculate VCN, we used the following formula: VCN = $VCN_{(standard\ curve)}$ * ng of "LV of interest" / ng of β-actin, where "LV of interest" is either HIV-gag or HSV-tk. The VCN of PGK:GFP LV was obtained by subtracting the VCN of HSV-tk from the total HIV-gag VCN.

STATISTICS: The data were represented as mean ± SEM of the indicated number of measurements. Statistical significance was calculated by t test where indicated (Prism v4.0b), with $p<0.05$ considered statistically significant.

ADDITIONAL REFERENCES

1. Mazzone, M. et al. Heterozygous deficiency of PHD2 restores tumor oxygenation and inhibits metastasis via endothelial normalization. *Cell* **136**, 839-51 (2009).

2. Foo, S.S. et al. Ephrin-B2 controls cell motility and adhesion during blood-vessel-wall assembly. *Cell* **124**, 161-73 (2006).

3. Benedito, R. et al. The notch ligands Dll4 and Jagged1 have opposing effects on angiogenesis. *Cell* **137**, 1124-35 (2009).

4. Chen, L.W. et al. The two faces of IKK and NF-kappaB inhibition: prevention of systemic inflammation but increased local injury following intestinal ischemia-reperfusion. *Nat Med* **9**, 575-81 (2003).

5. Luttun A, T.M., Moons L, Wu Y, Angelillo-Scherrer A, Liao F, Nagy JA, Hooper A, Priller J, De Klerck B, Compernolle V, Daci E, Bohlen P, Dewerchin M, Herbert JM, Fava R, Matthys P, Carmeliet G, Collen D, Dvorak HF, Hicklin DJ, Carmeliet P. Revascularization of ischemic tissues by PlGF treatment, and inhibition of tumor angiogenesis, arthritis and atherosclerosis by anti-Flt1. *Nat Med* **8**, 831-840 (2002).

6. Carmeliet P, M.L., Luttun A, Vincenti V, Compernolle V, De Mol M, Wu Y, Bono F, Devy L, Beck H, Scholz D, Acker T, DiPalma T, Dewerchin M, Noel A, Stalmans I, Barra A, Blacher S, Vandendriessche T, Ponten A, Eriksson U, Plate KH, Foidart JM, Schaper W, Charnock-Jones DS, Hicklin DJ, Herbert JM, Collen D, Persico MG. Synergism between vascular endothelial growth factor and placental growth factor contributes to angiogenesis and plasma extravasation in pathological conditions. *Nat Med* **7**, 575-583 (2001).

7. Lutgens, E. et al. Biphasic pattern of cell turnover characterizes the progression from fatty streaks to ruptured human atherosclerotic plaques. *Cardiovasc Res* **41**, 473-9 (1999).

8. Jordan, B.F., Cron, G.O. & Gallez, B. Rapid monitoring of oxygenation by 19F magnetic resonance imaging: Simultaneous comparison with fluorescence quenching. *Magn Reson Med* **61**, 634-8 (2009).

9. Pfeffer, M.A. et al. Myocardial infarct size and ventricular function in rats. *Circ Res* **44**, 503-12 (1979).

10. Meerpohl, H.G., Lohmann-Matthes, M.L. & Fischer, H. Studies on the activation of mouse bone marrow-derived macrophages by the macrophage cytotoxicity factor (MCF). *Eur J Immunol* **6**, 213-7 (1976).

11. De Palma, M. et al. Tumor-targeted interferon-alpha delivery by Tie2-expressing monocytes inhibits tumor growth and metastasis. *Cancer Cell* **14**, 299-311 (2008).

SUPPLEMENTARY TABLES

SUPPLEMENTARY TABLE 1: GENE EXPRESSION IN WT AND PHD2$^{+/-}$ ENDOTHELIAL CELLS.

	WT		PHD2$^{+/-}$	
GENE	**BASELINE**	**LIGATED**	**BASELINE**	**LIGATED**
Phd2	1 ± 0.16	1.2 ± 0.17	0.5 ± 0.03 *	0.5 ± 0.09 *
Tie2	1 ± 0.02	1.1 ± 0.39	1.1 ± 0.13	0.9 ± 0.40
Ang1	1 ± 0.25	1 ± 0.5	1.25 ± 0.5	1.25 ± 0.75
Ang2	1 ± 0.19	1.5 ± 0.05 #	1.04 ± 0.09	1.5 ± 0.16 #
Cxcl1	1 ± 0.38	2.5 ± 0.71	1.3 ± 0.29	2.8 ± 0.80
Cxcl2	n.d.		n.d.	
Cxcr4	1 ± 0.11	0.6 ± 0.11 #	0.9 ± 0.17	0.5 ± 0.08 #
Cx3cr1	1 ± 0.13	0.6 ± 0.13	0.9 ± 0.13	0.6 ± 0.11
hgf	1 ± 0.01	1.2 ± 0.36	1.2 ± 0.11	1.0 ± 0.25
Pdgfb	1 ± 0.06	0.9 ± 0.08	0.9 ± 0.15	0.9 ±0 .19
Plgf	1 ± 0.16	3.1 ± 0.84	1.5 ± 0.38	3.3 ± 0.56
Rantes	n.d.		n.d.	
Ccl17	n.d.		n.d.	
Ccl22	n.d.		n.d.	
Flk1	1 ± 0.14	0.4 ± 0.09 #	0.86 ± 0.09	0.4 ± 0.04 #
Flt1	1 ± 0.26	0.7 ± 0.17	0.9 ± 0.47	0.7 ± 0.24
sFlt1	1 ± 0.10	0.7 ± 0.03	1.0 ± 0.10	0.7 ± 0.12
Nrp1	1 ± 0.04	0.4 ± 0.08 #	0.9 ± 0.38	0.5 ± 0.05 #
Cdh5	1 ± 0.06	0.8 ± 0.06	1.2 ± 0.17	0.8 ± 0.17
Vegfa	1 ± 0.5	1 ± 0.30	0.8 ± 0.20	1.2 ± 0.20
Mmp2	1 ± 0.30	1.5 ± 0.42	1.2 ±0.37	1.4 ± 0.36
Mmp9	1 ± 0.48	0.6 ± 0.26	1.2 ±0.68	0.5 ± 0.11
Sdf1	1 ± 0.12	1.2 ± 0.26	0.8 ±0.12	1,0 ± 0.22
Tgfβ	1 ± 0.04	0.8 ± 0.05	0.9 ±0.09	1.0 ± 0.38
IL1β	n.d.		n.d.	

IL6	1 ± 0.23	1.6 ± 0.28	1.1 ± 0.14	1.72 ± 0.31
Nos3	1 ± 0.17	0.8 ± 0.11	0.8 ± 0.16	0.8 ± 0.14
Mcp1	1 ± 0.18	5.4 ± 0.13 #	0.9 ± 0.16	6.0 ±0.13 #
Tnfα	1 ± 0.21	0.8 ± 0.28	1.0 ± 0.18	0.7 ± 0.15
Cxcl10	1 ± 0.23	2.1 ± 0.19 #	1.1 ± 0.41	2.4 ± 0.27 #
IL12α	n.d.		n.d.	
IFNβ	n.d.		n.d.	
Cox2	1 ± 0.12	1.2 ± 0.04	1.1 ± 0.2	1.1 ± 0.2
Jagged1	1 ± 0.09	0.9 ± 0.07	1.1 ± 0.10	1.0 ± 0.15
Icam1	1 ± 0.11	0.8 ± 0.13	0.8 ± 0.09	0.6 ± 0.08

The data represent the expression analysis of endothelial cells, freshly sorted from WT and PHD2$^{+/-}$ adductor muscles at baseline and 72 hours after femoral artery occlusion (N=4-8, P<0.05). Data are normalized towards the expression levels of WT ECs at baseline; n.d.= not determined. Asterisks denote statistical significance versus WT. Hash signs denote statistical significance compared to the baseline.

SUPPLEMENTARY TABLE 2: COLLATERALIZATION IN MICE HAPLODEFICIENT FOR PHD2 IN HEMATOPOIETIC CELLS AND/OR ENDOTHELIAL CELLS.

Donor	*PHD2*$^{Tie2Cre;wt/wt}$	*PHD2*$^{Tie2Cre;lox/wt}$	*PHD2*$^{Tie2Cre;wt/wt}$	*PHD2*$^{Tie2Cre;lox/wt}$
Recipient	*PHD2*$^{Tie2Cre;wt/wt}$	*PHD2*$^{Tie2Cre;wt/wt}$	*PHD2*$^{Tie2Cre;lox/wt}$	*PHD2*$^{Tie2Cre;lox/wt}$
2nd generation collaterals	5.9 ± 1.0	13.3 ± 1.4 *#	8.2 ± 0.7	14.4 ± 1.6 *#
3rd generation collaterals	3.8 ± 0.7	7.2 ± 1.3 *#	2.7 ± 1.1	7.1 ± 1.0 *#

Reciprocal bone marrow transplantation in lethally irradiated mice reveals that the enhanced arteriogenesis of PHD2 heterozygous mice is specifically caused by loss of one PHD2 allele in bone marrow derived hematopoietic cells (green column) but not in endothelial cells (pink column) compared to WT controls (yellow column). Combined deletion of one PHD2 allele in both the hematopoietic and EC lineage (light blue column) does not modify the biological effect elicited on collateral arteries by PHD2 haplodeficient hematopoietic cells alone. Asterisks denote statistical significance versus *PHD2*$^{Tie2Cre;wt/wt}$ →*PHD2*$^{Tie2Cre;wt/wt}$. Hash signs denote statistical significance compared to *PHD2*$^{Tie2Cre;wt/wt}$ →*PHD2*$^{Tie2Cre;lox/wt}$.

SUPPLEMENTARY TABLE 3: HETEROZYGOUS DEFICIENCY OF PHD2 IN ENDOTHELIAL CELLS OR SMOOTH MUSCLE CELLS DOES NOT CONFER COLLATERAL PRECONDITIONING.

	PHD2$^{Cre;wt/wt}$		**PHD2$^{Cre;wt/lox}$**	
Promoter of Cre recombinase	2nd generation collaterals	3rd generation collaterals	2nd generation collaterals	3rd generation collaterals
VE-Cadherin	9.0 ± 0.6	10.8 ± 1.3	9.7 ± 1.1	11.0 ± 2.0
PDGFRB	8.2 ± 0.9	7.4 ± 1.4	7.2 ± 1.1	6.9 ± 1.6

The data represent the number of secondary (light grey column) and tertiary (light blue column) collateral branches in mice haplodeficient for PHD2 in ECs or SMCs at baseline. Mice carrying one floxed PHD2 allele were intercrossed with deleters expressing the Cre recombinase under an EC specific promoter, i.e. VE-Cadherin, or a SMC specific promoter, i.e. PDGFRB.

SUPPLEMENTARY TABLE 4: VECTOR COPY NUMBER IN BLOOD CELLS OF WT TIE2:TK-BMT AND PHD2$^{+/-}$ TIE2:TK-BMT MICE.

	HSV-tk	**HIV-gag**	**PGK:GFP**
WT Tie2:tk-BMT	8.93 ± 0.40	15.79 ± 0.02	6.85 ± 0.43
PHD2$^{+/-}$ Tie2:tk-BMT	10.53 ± 0.30	19.39 ± 0.01	8.85 ± 0.31

The data represent the number of integrated LV copies per cell genome (vector copy number, VCN ± SEM) of HSV-tk and HIV-gag in blood cells, collected at 4 weeks after transplantation from WT Tie2:tk-BMT and PHD2$^{+/-}$ Tie2:tk-BMT mice. The VCN of PGK:GFP was obtained by subtracting the VCN of HSV-tk from the total HIV-gag VCN (N=6; P=NS). See Experimental Methods for technical details.

SUPPLEMENTARY TABLE 5: LIST OF PRIMERS USED FOR RT-PCR.

GENE	PROBE	FORWARD	REVERSE
Nos2	ACT-ATA-ACT-CCA-TCA-AAA-GGA-GTG-GCT-CCC-AG	AGC-CCG-GGA-CTT-CAT-CAA-TC	TGA-AGC-CGC-TGC-TCA-TGA-G
Nos3	ACT-ATA-ACT-CCA-TCA-AAAGGA-GTG-GCT-CCC-AG	AGC-CCG-GGA-CTTCAT-CAA-TC	TGA-AGC-CGC-TGCTCA-TGA-G
Icam1	CCT-CAT-GCA-AGG-AGG-ACC-TCA-GCC-T	GTC-CGT-GCA-GGT-GAA-CTG-TTC	CTT-TCA-GCC-ACT-GAG-TCT-CCA-A
Pdgfb	CCC-ATC-TTC-AAG-AAG-GCC-ACA-GTG-ACC-T	CGG-TCC-AGG-TGA-GAA-AGA-TTG	CGT-CTT-GGC-TCG-CTG-CTC
Egln1/Phd2	ACG-AAA-GCC-ATG-GTT-GCT-TGT-TAC-CCA	GCT-GGG-CAA-CTA-CAG-GAT-AAA-C	CAT-AGC-CTG-TTC-GTT-GCC-T
Flt4	CGG-CGA-GCC-CCA-CTT-GTC-CA	GGT-TCC-TGA-TGG-GCA-AAG-G	TCA-GTG-GGC-TCA-GCC-ATA-GG
sFlt1	TTT-GCC-GCA-GTG-CTCACC-TCT-AAC-G	GAA-GAC-ATC-CTTCGG-AAG-CAC-GAA	TTG-GAG-ATC-CGAGAG-AAA-ATG-G
Cxcl12/Sdf1	CGG-TAA-ACC-AGT-CAG-CCT-GAG-CTA-CCG	CCG-CGC-TCT-GCAT-CAG-T	GCG-ATG-TGG-CTC-TCGAAG-A

Tgfβ	TGC-TAA-AGA-GGT-CAC-CCG-CGT-GCT	GAG-CCC-GAA-GCG-GAC-TAC-T	GCG-TTG-TTG-CGG-TCC-AC

For the following genes with sequence ID (enclosed between brackets), commercially available primers were ordered from Applied Biosystems (https://products.appliedbiosystems.com): ***Ang1*** (Mm00456498_m1), ***Ang2*** (Mm00545822_m1), ***Arg1*** (Mm00475991_m1), ***Calponin-1*** (Mm00487032_m1), ***Ccl17*** (Mm00516136_m1), ***Ccl22*** (Mm00436439_m1), ***Cox2*** (Mm00478374_m1), ***Cxcl1*** (Mm00433859_m1), ***Cxcl10*** (Mm99999072_m1), ***Cxcl2*** (Mm00436450_m1), ***Cx3cr1*** (Mm0262011_s1), ***Cxcr4*** (Mm01292123_m1), ***Fizz*** (Mm00445109_m1), ***Flt1*** (Mm01210866_m1), ***Hgf*** (Mm01135185_m1), ***Ifnβ*** (Mm00439552_s1), ***IL12α*** (Mm00434169_m1), ***IL1β*** (Mm01336189_m1), ***IL6*** (Mm01210733_m1), ***Mcp1*** (Mm00441242_m1), ***Mmp2*** (Mm00439506_m1), ***Mmp9*** (Mm00442991_m1), ***Nrp1*** (Mm01253210_m1), ***NmMHC*** (Mm00805131_m1), ***Egln2/Phd1*** (Mm00519067_m1), ***Egln3/Phd3*** (Mm00472200_m1), ***Plgf*** (Mm00435613_m1), ***Rantes*** (Mm01302428_m1), ***SM22α*** (Mm00441660_m1), **Smoothelin** (Mm00449973_m1), ***Tie2*** (Mm00443243_m1), ***Tnfα*** (Mm00443258_m1), ***Vegfa*** (Mm00437304_m1), Ym1 (Mm00657889_mH), ***αSMA*** (Mm01546133_m1), ***Jagged1*** (Mm00496902_m1), ***Flk1*** (Mm01222419_m1), ***Cdh5*** (Mm00486938_M1).

SUPPLEMENTARY NOTES

SUPPLEMENTARY NOTE 1: To measure the silencing of SDF1 and PDGFB, we performed RT-PCR on WT and $PHD2^{+/-}$ pMØ at 4 days after transduction with a lentiviral vector carrying an shRNA against SDF1 or PDGFB. Compared to their scramble control, the knockdown for SDF1 was 77 ± 5.0% and 71 ± 2.6%, and for PDGFB 81 ± 3.2% and 87 ± 5.9% in WT and $PHD2^{+/-}$ pMØ, respectively (N=4; P<0.01).

SUPPLEMENTARY NOTE 2: We also cotransduced WT and $PHD2^{+/-}$ bone marrow cells with a lentiviral vector ubiquitously expressing GFP under the PGK promoter, in order to measure bone marrow engraftment in the transplanted mice by scoring GFP expression. By using flow cytometry of GFP^+ cells and RT-PCR analysis of integrated vectors in blood cells, we found that PHD2 haplodeficiency in bone marrow hematopoietic cells did not preclude their full engraftment upon transplantation in irradiated mice (GFP^+ cells, % of leukocyte population: 92.6 ± 2.5% in WT Tie2:tk-BMT mice and 89.3 ± 5.5% in $PHD2^{+/-}$ Tie2:tk-BMT mice; N=6; P=NS; and Supplementary Table 4).

SUPPLEMENTARY NOTE 3: Four weeks after transplantation, WT and $PHD2^{+/-}$ Tie2:tk-BMT mice were treated with either saline or GCV (50 mg/kg daily) for ten days before and three days after femoral artery ligation. The depletion of TEMs was assessed by F4/80 and Tie2 double staining of baseline and ligated adductor sections. We found that GCV treatment reduced the density of $F4/80^+Tie2^+$ cells by 46 ± 10% in WT Tie2:tk-BMT mice and 58 ± 11% in $PHD2^{+/-}$ Tie2:tk-BMT mice at baseline (N=6; P<0.001), and by 39 ± 6% in WT Tie2:tk-BMT mice and 68 ± 5% in $PHD2^{+/-}$ Tie2:tk-BMT mice 3 days post-ligation (N=6; P<0.001); similar levels of TEM depletion were obtained at 7 days post-ligation carrying on the GCV treatment for the entire period of ischemia (not shown).

SUPPLEMENTARY NOTE 4: To address whether the induction of PHD3 rescued the activation of NF-κB pathway by loss of PHD2, we silenced PHD3 in $PHD2^{LysCre;wt/wt}$, $PHD2^{LysCre;lox/wt}$ and $PHD2^{LysCre;lox/lox}$ macrophages carrying the NF-κB-responsive

luciferase reporter. The knockdown of PHD3 was 63 ± 0.03%, 60 ± 0.04%, and 37 ± 0.01% in $PHD2^{LysCre;wt/wt}$, $PHD2^{LysCre;lox/wt}$, and $PHD2^{LysCre;lox/lox}$ macrophages, respectively, compared to their scramble controls (N=4; P<0.001).

SUPPLEMENTARY NOTE 5: To dissect the axis of NF-κB activation in $PHD2^{+/-}$ macrophages, we silenced the main components of the canonical pathway, i.e. p65 (RelA) and p50 (NF-κB1) in macrophages carrying the NF-κB-responsive luciferase reporter. The efficiency of knockdown for p65 was 52.7% ± 1.4% and 50.2% ± 0.4% in WT and $PHD2^{+/-}$ macrophages compared to their scramble control. Respectively, the efficiency of knockdown for p50 was 49.6% ± 0.9% and 59.1% ± 1.2% in WT and $PHD2^{+/-}$ macrophages compared to their scramble control (N=4, p<0.001).

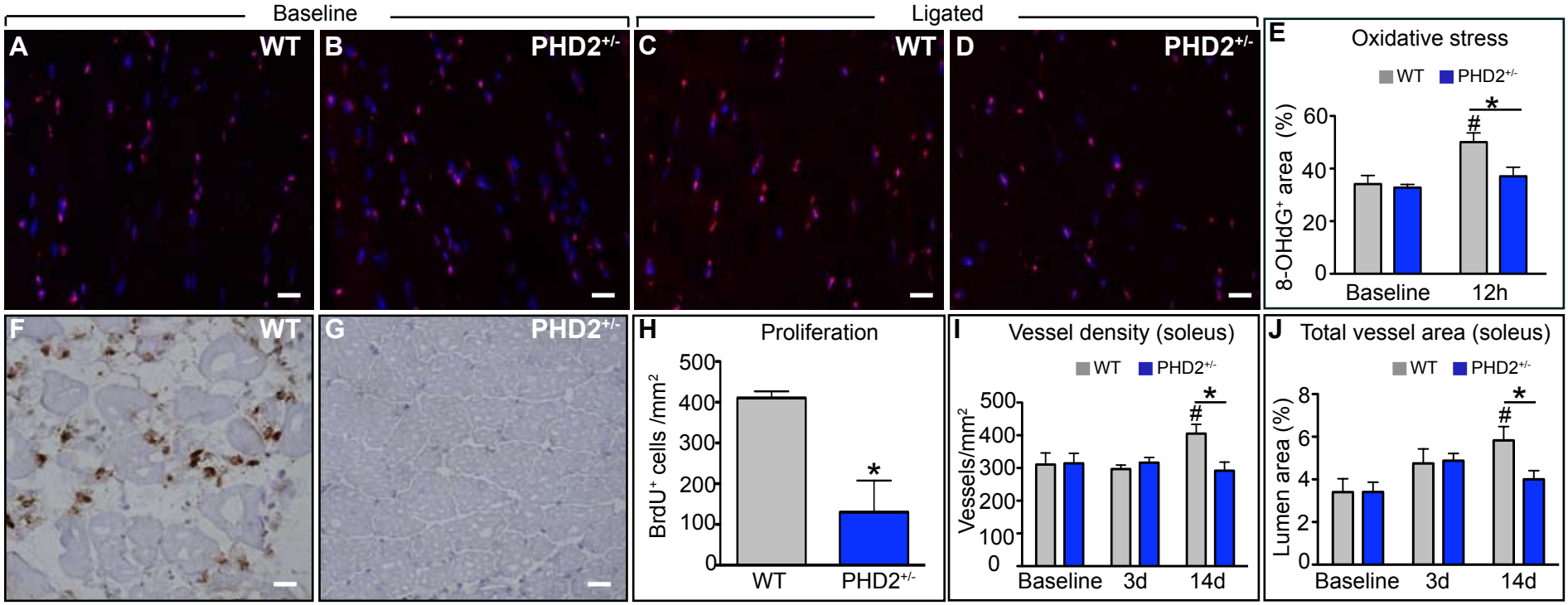

SUPPLEMENTARY FIGURE 1: PHD2 HAPLODEFICIENCY PREVENTS ISCHEMIC DAMAGE

A-D, Staining for 8-hydroxy-2-deoxyguanosine (8-OHdG; red) and cell nuclei (DAPI, blue) in WT and PHD2$^{+/-}$ crural muscles before and after ischemia (12h). At baseline, 8-OHdG^{+} area is similar in both genotypes (A,B). After occlusion, WT (C), but not PHD2$^{+/-}$ crural muscles present enhanced oxidative stress. **E,** Quantification of the 8-OHdG^{+} area represented in A-D (N=8; P=0.02). **F,G,** Cell proliferation assessed by BrdU immunostaining indicates reduced muscle regeneration in PHD2$^{+/-}$ mice (G) 72 hours post-ischemia. **H,** Quantification of BrdU^{+} cells in the crural muscle represented in F,G (N=3; P=0.02). **I, J,** Vessel density (I) and area (J) at baseline and after femoral artery ligation in the soleus of WT and PHD2$^{+/-}$ mice (N=5-8; P<0.05). Scale bars denote 20 μm in A,B,C,D,F and G. Asterisk in E,H,I, and J denotes statistical significance (P<0.05) compared to WT. Hash signs in E,I, and J denote statistical significance (P<0.05) towards baseline.

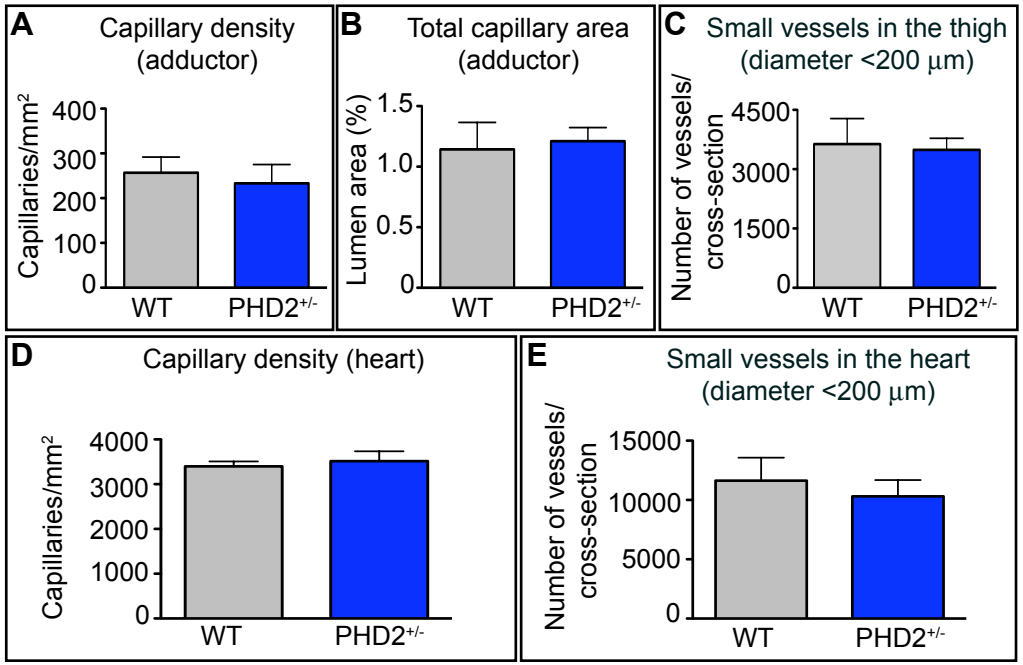

SUPPLEMENTARY FIGURE 2: PHD2 HAPLODEFICIENCY DOES NOT AFFECT CAPILLARY VESSELS

A,B, Capillary density (A) and total capillary area (B) in the adductor of WT and PHD2$^{+/-}$ mice at baseline (N=8; P=NS). **C,** Number of small vessels (<200 μm in diameter) in the thigh of non-ligated WT and PHD2$^{+/-}$ mice by micro-CT angiography (N=6; P=NS). **D,** Capillary density in WT and PHD2$^{+/-}$ hearts at baseline (N=5; P=NS). **E,** Number of small vessels (<200 μm in diameter) in WT and PHD2$^{+/-}$ hearts at baseline by micro-CT angiography (N=5; P=NS).

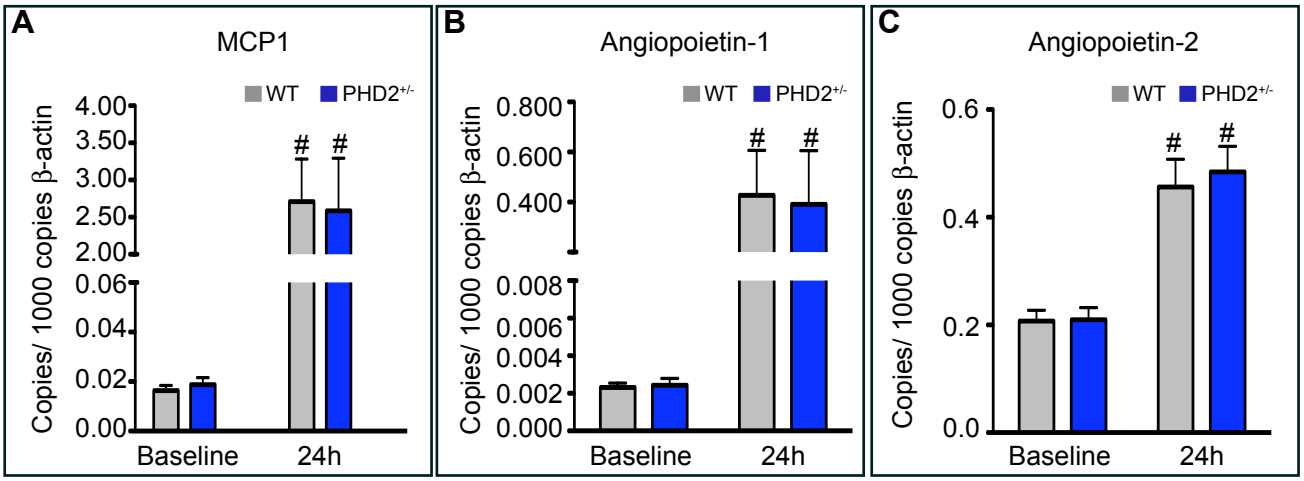

SUPPLEMENTARY FIGURE 3: PHD2 HAPLODEFICIENCY DOES NOT CHANGE THE EXPRESSION OF CHEMOATTRACTANTS

A-C, Histograms showing comparable expression (qRT-PCR) of MCP1 (A), angiopoietin-1 (B) and angiopoietin-2 (C) in adductor muscles of non-ligated and ligated WT and PHD2$^{+/-}$ mice (N=6-18; P=NS). MCP1, angiopoietin-1 and angiopoietin-2 levels increased after ligation and were comparable in both genotypes (N=6-18; P<0.005). Hash signs in A, B and C denote statistical significance (P<0.05) versus baseline.

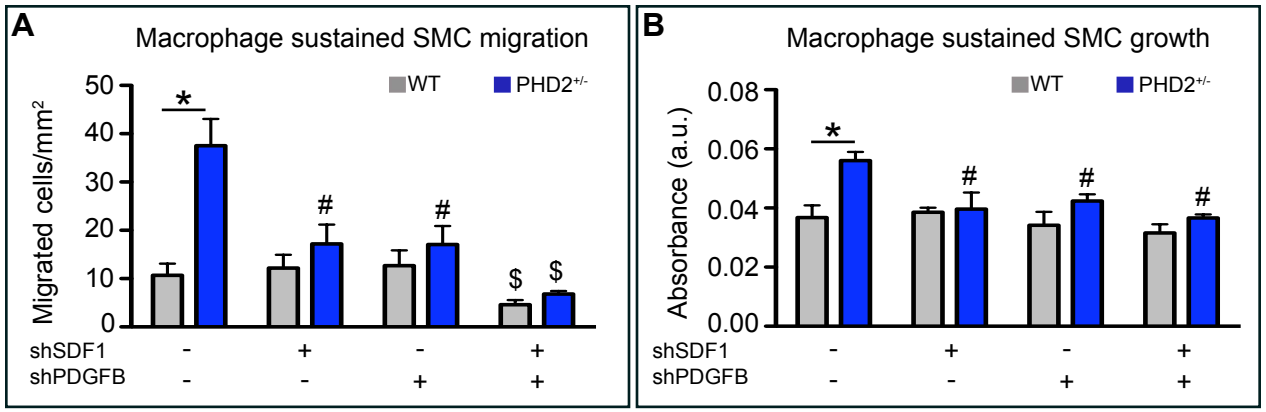

SUPPLEMENTARY FIGURE 4: SILENCING OF SDF1 AND PDGFB IN PHD2$^{+/-}$ MACROPHAGES REDUCES SMC MIGRATION AND GROWTH IN VITRO

A,B, WT and PHD2$^{+/-}$ macrophages were transduced with lentiviral vectors carrying a shRNA against SDF1 or PDGFB. **A,** Knock-down of SDF1 or PDGFB alone abrogates SMC migration induced by PHD2$^{+/-}$ macrophages, whereas combined silencing is more effective (N=7-12; P<0.05). **B,** Single knockdown of SDF1 or PDGB decreases SMC growth induced by PHD2$^{+/-}$ macrophages. However, the combined silencing does not have an additive effect. A scramble shRNA was used as control in A,B. Asterisk denotes statistical significance versus WT. Hash signs denote statistical significance towards scramble. Dollar signs denote statistical significance towards the baseline and either treatment alone.

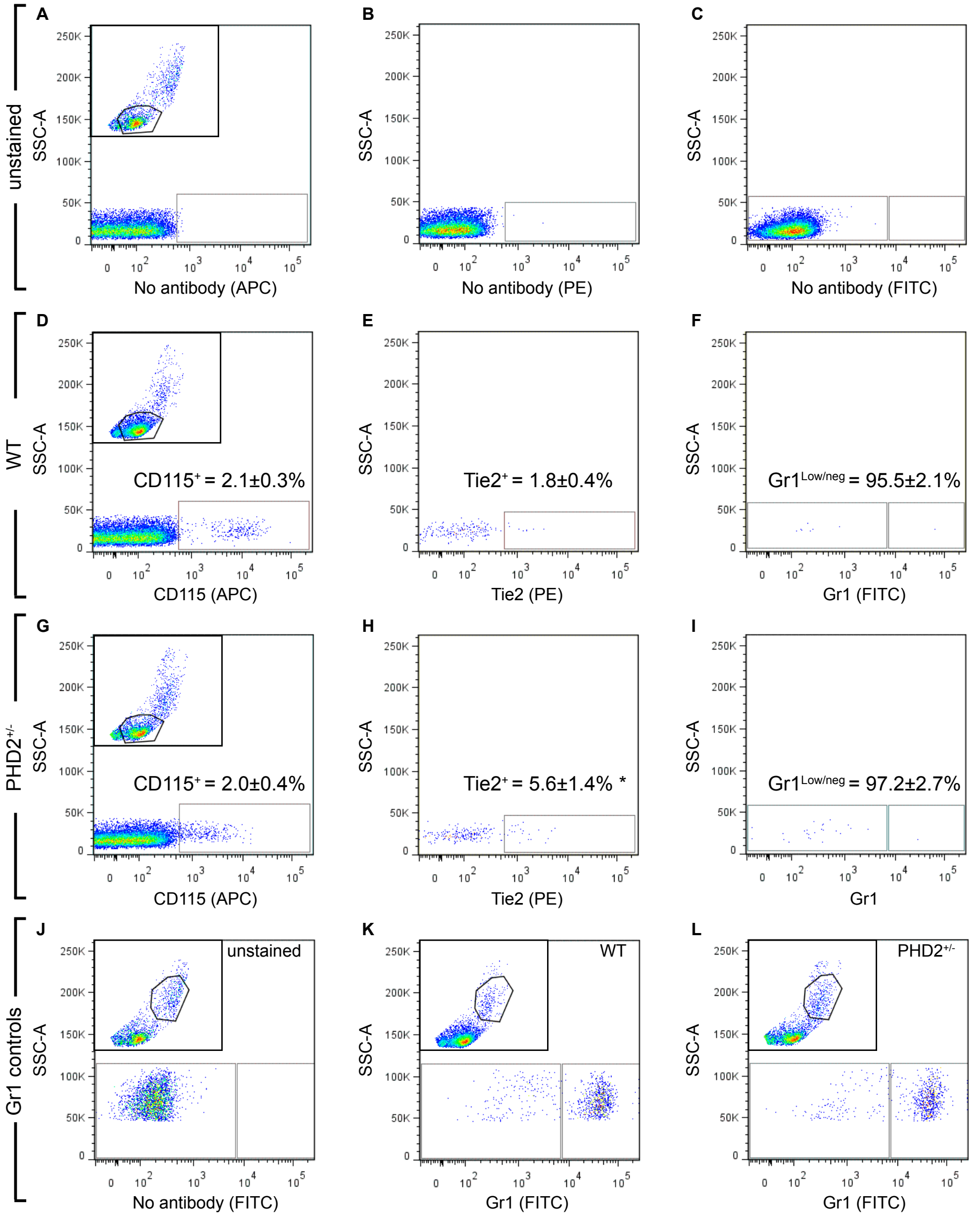

SUPPLEMENTARY FIGURE 5: FLOW CYTOMETRIC ANALYSIS OF CIRCULATING MONOCYTES

A-C, Blood mononuclear cells from WT mice were gated as in the inset in A, and autofluorescence of the gated cells was analyzed using the APC, PE and FITC channels. **D-F,** Blood mononuclear cells from WT mice were gated as in the inset in D and analyzed for the expression of the monocyte marker CD115 (D). $CD115^{+}$ monocytes (gate in D) were then analyzed for the expression of Tie2 (E). $CD115^{+}Tie2^{+}$ TEMs (gate in E) were further analyzed for the expression of Gr1 (F). **G-I,** Blood mononuclear cells from $PHD2^{+/-}$ mice were gated as in the inset in G and analyzed as in D-F above. **J-L,** Neutrophils were identified by their light scattering features and gated as in the insets. Expression of Gr1 was then analyzed in the gated cells from either WT (K) or $PHD2^{+/-}$ (L) mice, and used as $Gr1^{high}$ reference in F,I; the unstained control is represented in J. Asterisk in H denotes statitstical significance towards WT (N=14; P=0.01).

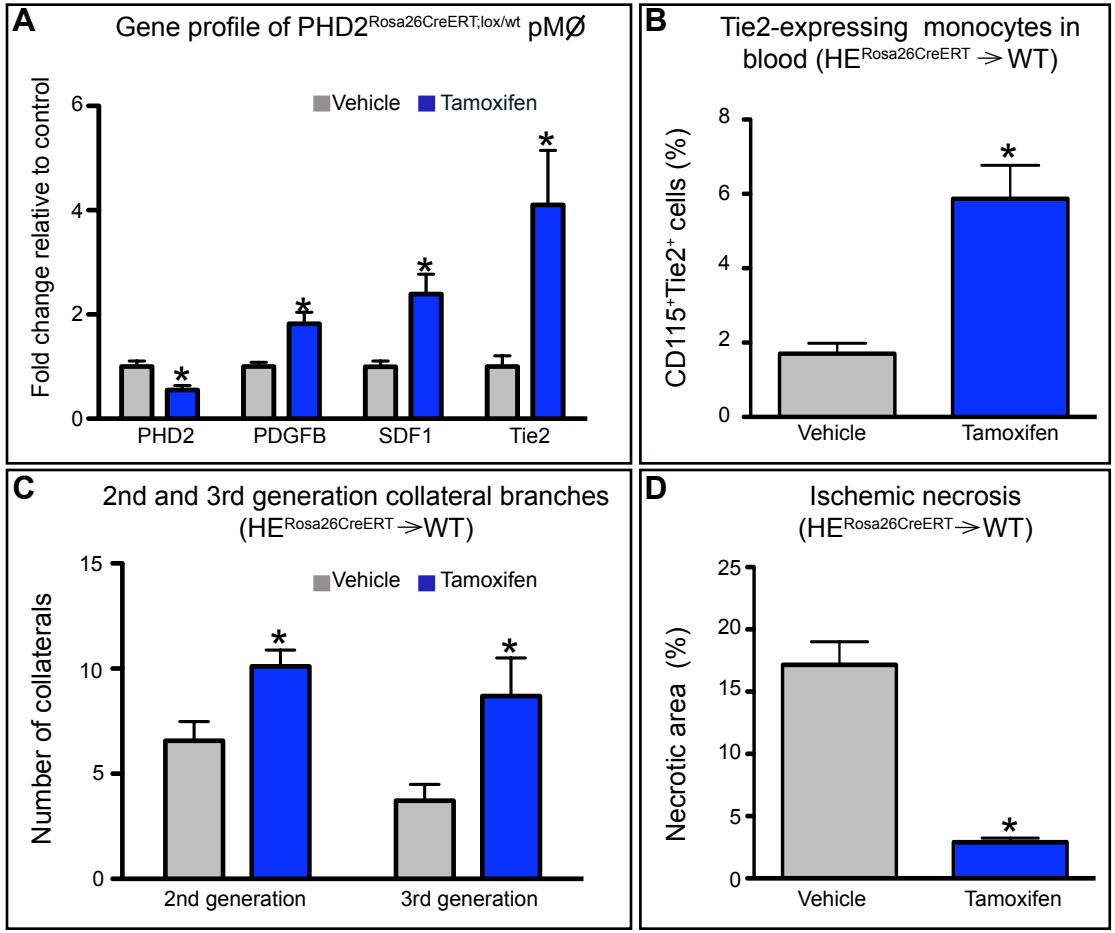

SUPPLEMENTARY FIGURE 6: ACUTE DELETION OF ONE PHD2 ALLELE PROMOTES ARTERIOGENIC MACROPHAGES

A, PHD2$^{Rosa26CreERT;lox/wt}$ peritoneal macrophages treated with 2 μM 4-hydroxytamoxifen for 48 hours present increased expression of PDGFB, SDF1, and Tie2 resembling the phenotype of PHD2$^{+/-}$ macrophages (N=4; P<0.05). **B,** WT mice transplanted with the bone marrow of PHD2$^{Rosa26CreERT;lox/wt}$ mice (HE^{Rosa26CreERT} → WT) present increased number of Tie2^{+} circulating monocytes (CD115^{+}Tie2^{+} double positive cells) after tamoxifen treatment (N=6; P<0.01). **C,** Tamoxifen treated HE^{Rosa26CreERT} → WT mice present increased number of 2nd and 3rd generation collateral vessels compared to untreated mice at baseline (N=10-14; P<0.01). **D,** 72 hours after femoral artery ligation, tamoxifen treated HE^{Rosa26CreERT} → WT mice present reduced necrotic area compared to untreated animals. Asterisks in A,B,C, and D denote statistical significance (P<0.05) compared to untreated HE^{Rosa26CreERT} → WT mice.

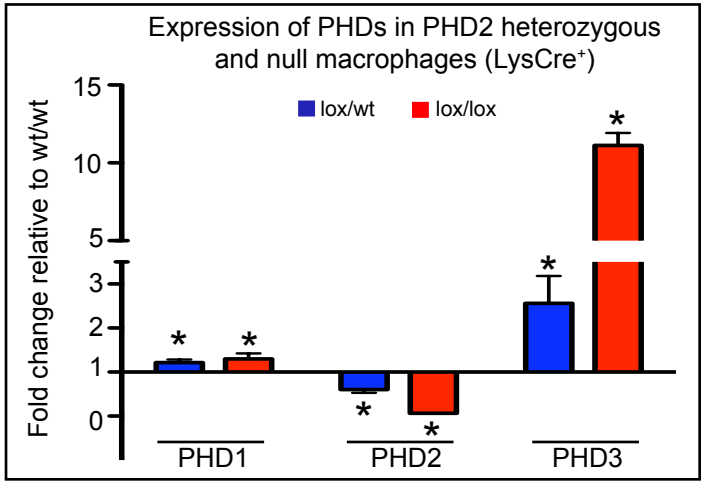

SUPPLEMENTARY FIGURE 7: PHD EXPRESSION IN PHD2 HETEROZYGOUS AND PHD2 NULL MACROPHAGES

RNA levels of PHD1, PHD2, and PHD3 in macrophages from $PHD2^{LysCre;wt/wt}$, $PHD2^{LysCre;lox/wt}$, and $PHD2^{LysCre;lox/lox}$ (labeled as wt/wt, lox/wt, and lox/lox respectively) mice. As expected, PHD2 levels were significantly decreased in $PHD2^{LysCre;lox/wt}$ and $PHD2^{LysCre;lox/lox}$ macrophages. PHD1 and PHD3 transcript levels were higher in PHD2 heterozygous and null macrophages (N=4; $P<0.01$). Asterisks denote statistical significance ($P<0.05$) compared to wt/wt macrophages.

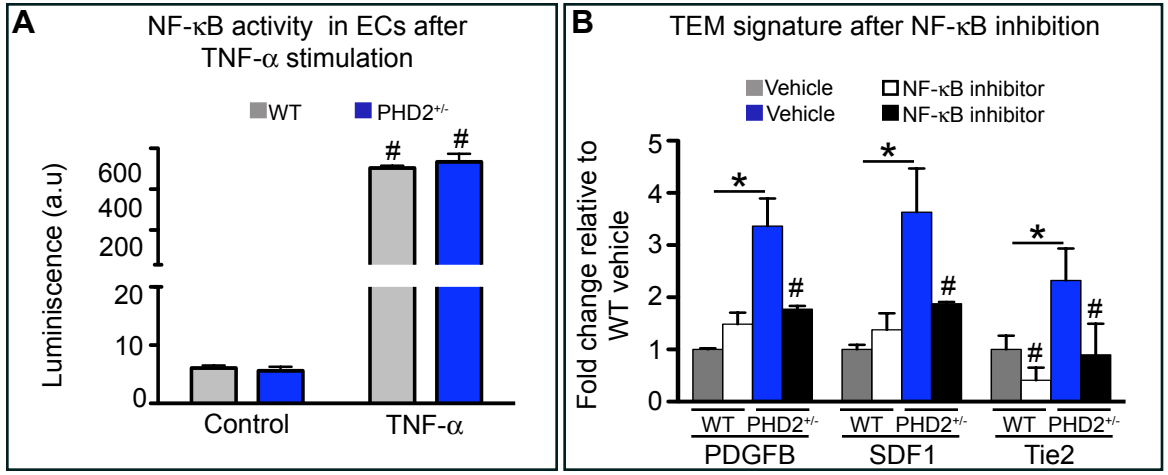

SUPPLEMENTARY FIGURE 8: NF-KB IS SELECTIVELY ACTIVATED IN PHD2$^{+/-}$ MACROPHAGES

A, Histogram showing comparable NF-κB activity in WT and PHD2$^{+/-}$ ECs at baseline; stimulation with TNF-α (20 ng/mL, 8 hours) unleashes NF-κB activity to the same level in both genotypes (N=4, P< 0.05). **B,** Pharmacological inhibition of NF-κB activity reduces the expression of PDGFB, SDF1 and Tie2 in PHD2 haplodeficient macrophages (N=3-8; P<0.05). Asterisks denote statistical significance (P<0.05) compared to WT vehicle treated macrophages. Hash signs denote statistical significance compared to control in A or to WT vehicle in B.

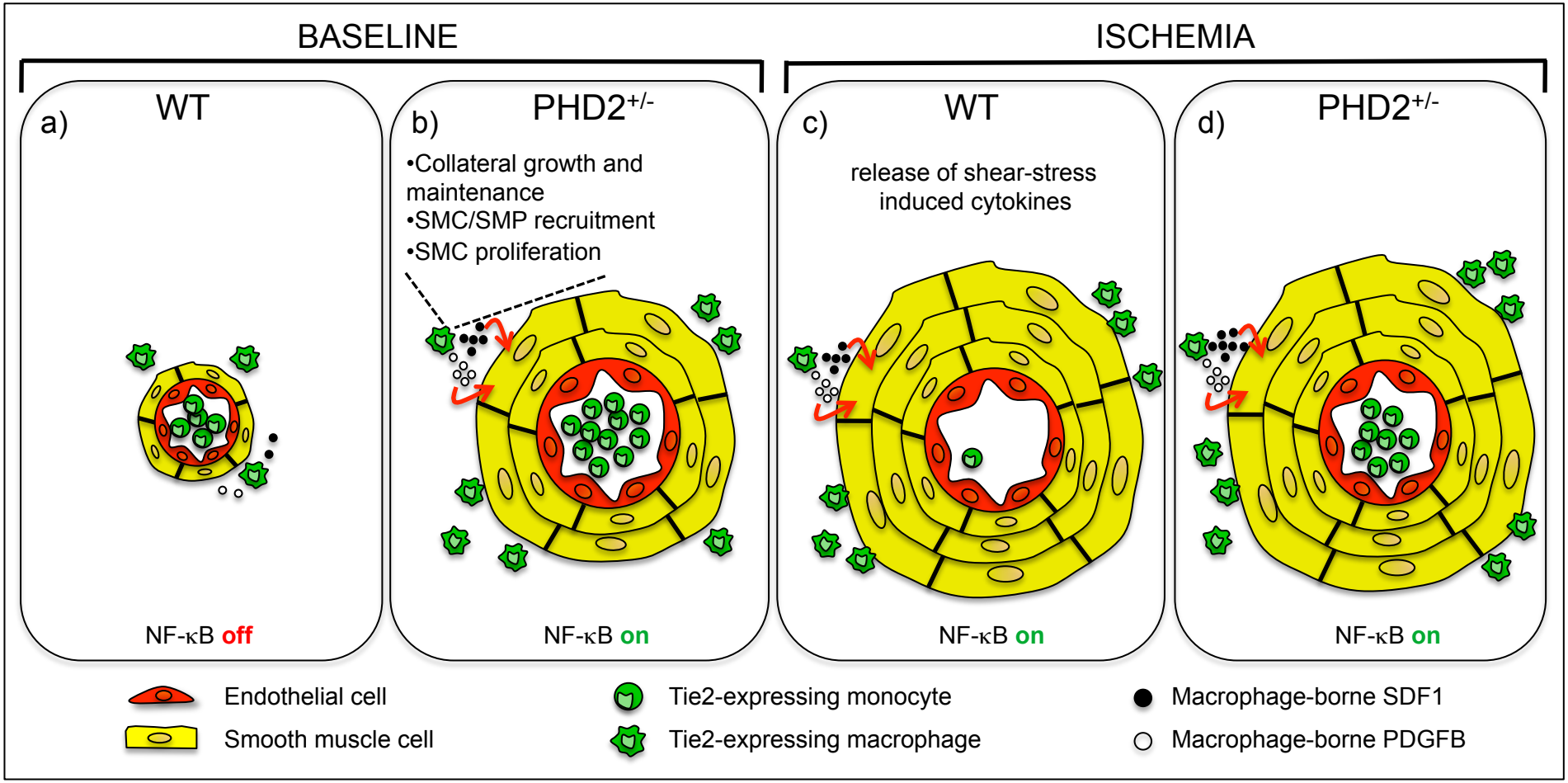

SUPPLEMENTARY FIGURE 9: SCHEME OF COLLATERAL ARTERIAL GROWTH IN WT AND PHD2$^{+/-}$ MICE

Collateral vessels are preexisting small conduits (shown in panel a) that undergo growth and maturation in case of occlusion of the major arterial flow, a process named arteriogenesis. PHD2$^{+/-}$ mice are preadapted to ischemia and display enhanced collateralization at baseline (panel b). The absence of one PHD2 allele in monocytes unleashes NF-κB signals that expand the reservoir of Tie2-expressing monocytes (TEMs) in the blood. Once extravasated into the pericollateral region, they differentiate into Tie2-expressing macrophages and promote collateral vessel maturation and homeostasis. SDF1 and PDGFB production by TEMs induces smooth muscle cell/progenitor recruitment and proliferation, ultimately leading to more abundant, larger, thicker, mature, and functional collateral arteries. In ischemia, shear stress-induced cytokines recruit circulating TEMs in WT mice (panel c). Tissue infiltrating TEMs foster arteriogenesis in a NF-κB dependent fashion and newly formed collateral arteries will partly reestablish blood flow. In PHD2$^{+/-}$ mice, femoral artery occlusion also induces extravasation and recruitment of TEMs, but to a lower extent (panel d), likely because of their collateral vessel preconditioning at baseline.